Profiles of the Unitarity Triangle and CP-Violating Phases in the Standard Model and Supersymmetric Theories

A. Ali

Deutsches Elektronen Synchrotron DESY, Hamburg

and

D. London

Laboratoire René J.-A. Lévesque, Université de Montréal, C.P. 6128, succ. centre-ville, Montréal, QC, Canada H3C 3J7

Abstract

We report on a comparative study of the profile of the CKM unitarity triangle, and the resulting CP asymmetries in B decays, in the standard model and in several variants of the minimal supersymmetric standard model (MSSM), characterized by a single phase in the quark flavour mixing matrix. The supersymmetric contributions to the mass differences ΔM_d, ΔM_s and to the CP-violating quantity $|\epsilon|$ are, to an excellent approximation, equal to each other in these theories, allowing for a particularly simple way of implementing the resulting constraints on the elements of V_{CKM} from the present knowledge of these quantities. Incorporating the next-to-leading-order corrections and applying the current direct and indirect constraints on the supersymmetric parameters, we find that the predicted ranges of $\sin 2\beta$ in the standard model and in MSSM models are very similar. However, precise measurements at B-factories and hadron machines may be able to distinguish these theories in terms of the other two CP-violating phases α and γ. This is illustrated for some representative values of the supersymmetric contributions in ΔM_d, ΔM_s and $|\epsilon|$.

arXiv:hep-ph/9903535v2 21 Apr 1999

η

(ρ,η)

$\dfrac{V_{ub}^{*}}{\lambda V_{cb}}$ 　　α 　　 $\dfrac{V_{td}}{\lambda V_{cb}}$

γ 　　　　　　　 β

(0,0) 　　　　　　　　　 (1,0) 　ρ

Figure 1: The unitarity triangle. The angles α, β and γ can be measured via CP violation in the B system.

1 Introduction

Within the standard model (SM), CP violation is due to the presence of a nonzero complex phase in the Cabibbo-Kobayashi-Maskawa (CKM) quark mixing matrix V [1]. A particularly useful parametrization of the CKM matrix, due to Wolfenstein [2], follows from the observation that the elements of this matrix exhibit a hierarchy in terms of λ, the Cabibbo angle. In this parametrization the CKM matrix can be written approximately as

$$
V \simeq \begin{pmatrix} 1 - \frac{1}{2}\lambda^2 & \lambda & A\lambda^3\left(\rho - i\eta\right) \\ -\lambda(1 + iA^2\lambda^4\eta) & 1 - \frac{1}{2}\lambda^2 & A\lambda^2 \\ A\lambda^3\left(1 - \rho - i\eta\right) & -A\lambda^2 & 1 \end{pmatrix} . \tag{1}
$$

The allowed region in ρ–η space can be elegantly displayed using the so-called unitarity triangle (UT). The unitarity of the CKM matrix leads to the following relation:

$$
V_{ud}V_{ub}^{*} + V_{cd}V_{cb}^{*} + V_{td}V_{tb}^{*} = 0 . \tag{2}
$$

Using the form of the CKM matrix in Eq. (1), this can be recast as

$$
\frac{V_{ub}^{*}}{\lambda V_{cb}} + \frac{V_{td}}{\lambda V_{cb}} = 1 , \tag{3}
$$

which is a triangle relation in the complex plane (i.e. ρ–η space), illustrated in Fig. 1. Thus, allowed values of ρ and η translate into allowed shapes of the unitarity triangle.

Constraints on ρ and η come from a variety of sources. Of the quantities shown in Fig. 1, $|V_{cb}|$ and $|V_{ub}|$ can be extracted from semileptonic B decays, while $|V_{td}|$ is probed in B_d^0–$\overline{B_d^0}$ mixing. The interior CP-violating angles α, β and γ can be measured through CP asymmetries in B decays [3]. Additional constraints come from CP violation in the kaon system ($|\epsilon|$), as well as B_s^0–$\overline{B_s^0}$ mixing.

In light of the fact that the B-factory era is almost upon us, one of the purposes of this paper is to update the profile of the unitarity triangle within the SM using the latest experimental

data. This analysis is done at next-to-leading-order (NLO) precision, taking into account the state-of-the-art calculations of the hadronic matrix elements from lattice QCD and available data. This therefore provides a theoretically-robust overview of the SM expectations for the allowed values of the CP-violating phases, as well as their correlations.

These CP phases are expected to be measured in the very new future. If Nature is kind, the unitarity triangle, as constructed from direct measurements of α, β and γ, will be inconsistent with that obtained from independent measurements of the sides. If this were to happen, it would be clear evidence for the presence of physics beyond the SM, and would be most exciting.

One type of new physics which has been extensively studied is supersymmetry (SUSY). There are a number of hints suggesting that SUSY might indeed be around the corner. One example is gauge-coupling unification: a supersymmetric grand unified theory does better than its non-supersymmetric counterpart. (How compelling these hints are depends on one's point of view.) Partly motivated by this success, but mostly on theoretical grounds, a great deal of effort has gone into a systematic study of the pattern of flavour violation in SUSY, where a number of flavour-changing neutral-current processes in K and B decays have been studied. In this paper we investigate the profile of the unitarity triangle in supersymmetric models. In particular, we explore the extent to which SUSY can be discovered through measurements of the sides and angles of the unitarity triangle.

If new physics (of any type) is present, the principal way in which it can enter is via new contributions, possibly with new phases, to K^0–$\overline{K^0}$, B_d^0–$\overline{B_d^0}$ and B_s^0–$\overline{B_s^0}$ mixing [4]. The decay amplitudes, being dominated by virtual W exchange, remain essentially unaffected by new physics. Thus, even in the presence of new physics, the measured values of $|V_{cb}|$ and $|V_{ub}|$ correspond to their true SM values, so that two sides of the UT are unaffected (see Fig. 1). However, the third side, which depends on $|V_{td}|$, will in general be affected by new physics. Furthermore, the measurements of $|\epsilon|$ and B_s^0–$\overline{B_s^0}$ mixing, which provide additional constraints on the UT, will also be affected. Therefore, if new physics is present, the allowed region of the UT, as obtained from current experimental data, may not correspond to the true (SM) allowed region.

The CP angles α and β are expected to be measured via CP-violating asymmetries in $B_d^0(t) \to \pi^+\pi^-$ and $B_d^0(t) \to J/\Psi K_s$, respectively [3]. If there is new physics in B_d^0–$\overline{B_d^0}$ mixing, *with new phases*, then these measurements will be affected. On the other hand, if there are no new phases, then the measurements will probe the true SM values. The third angle γ can be measured in a variety of ways. If it is obtained from a CP asymmetry involving a neutral B meson (B_d^0 or B_s^0), then it may be affected by new physics. However, if it is measured via charged B decays, then the measured value will correspond to the true (SM) value.

The most general SUSY models allow for the presence of new phases in the couplings of supersymmetric and ordinary particles. In such models the new phases are essentially unconstrained, so that the measured CP phases can be greatly shifted from their SM values. If this is the case, then the new physics will be relatively easy to find: the unitarity triangle constructed from the measurements of α, β and γ will be considerably different from that constructed from measurements of the sides. However, precisely because these new phases are unconstrained, these models lack predictivity. All that one can say is that there are regions of parameter space in which large effects are possible. (Indeed, this is true for any model of new physics

which allows for new phases. Examples include models with four generations, Z-mediated flavour-changing neutral currents, flavour-changing neutral scalars, etc. [5].)

In part because of this, most of the theoretical attention has focussed on SUSY models which, though less general, have considerably more predictive power. The most theoretically-developed model is the minimal supersymmetric standard model (MSSM). Although this is often referred to as a single model, in point of fact there are several variants of the MSSM. Among these is the scenario of minimal supersymmetric flavour violation [6], which involves, in addition to the SM degrees of freedom, charged Higgs bosons, a light stop (assumed right-handed) and a light chargino, with all other degrees of freedom assumed heavy and hence effectively integrated out. This scenario can be embedded in supergravity (SUGRA) models with gauge-mediated supersymmetry breaking, in which the first two squark generations and the gluinos are assumed heavy. Regardless of which variant is used, the key point for our purposes is that there are no new phases in the couplings – although there are many new contributions to meson mixing, all are proportional to the same combination of CKM matrix elements as found in the SM. As explained above, in this class of models measurements of the CP phases will yield the true SM values for these quantities. However, measurements of meson mixing will be affected by the presence of this new physics.

In this minimal SUSY scenario, NLO calculations for ΔM_d, ΔM_s and $|\epsilon|$ can be extracted from the work of Krauss and Soff [7]. Also, NLO corrections to the decay $B \to X_s \gamma$ have been worked out by Ciuchini et al. [6]. We make use of this work and present the profile of the unitarity triangle and CP-violating phases in this scenario, at the NLO precision. A particularly nice feature is that the SUSY contributions to K^0–$\overline{K^0}$, B_d^0–$\overline{B_d^0}$ and B_s^0–$\overline{B_s^0}$ mixing have the same form. Thus, as far as the unitarity triangle is concerned, the various SUSY models can be distinguished by a single parameter, f. This simplifies the analysis considerably.

We note that bits and pieces of such an analysis are already present in the literature. However, a theoretically-consistent analysis of the CKM unitarity triangle and the CP-violating phases, taking into account all constraints, has not been performed yet, to the best of our knowledge.

With this analysis, one can explore the extent to which the presence of minimal supersymmetry can be discovered through the precision measurements of the unitarity triangle which will be undertaken by experiments at the B-factories and hadron colliders. As we will see, the profiles of the unitarity triangle in the SM and in MSSM models are similar. However, precise measurements may be able to distinguish them.

In Section 2, we discuss the profile of the unitarity triangle within the SM. We describe the input data used in the fits and present the allowed region in ρ–η space, as well as the presently-allowed ranges for the CP angles α, β and γ. We turn to supersymmetric models in Section 3. We review several variants of the MSSM, in which the new phases are essentially zero. We also discuss the NLO corrections in such models and show that the SUSY contributions to K^0–$\overline{K^0}$, B_d^0–$\overline{B_d^0}$ and B_s^0–$\overline{B_s^0}$ mixing are of the same form and can be characterized by a single parameter f. We compare the profile of the unitarity triangle in SUSY models, for various values of f, with that of the SM. We conclude in Section 4.

2 Unitarity Triangle: SM Profile

2.1 Input Data

The CKM matrix as parametrized in Eq. (1) depends on four parameters: λ, A, ρ and η. We summarize below the experimental and theoretical data which constrain these CKM parameters.

- $|V_{us}|$: We recall that $|V_{us}|$ has been extracted with good accuracy from $K \to \pi e \nu$ and hyperon decays [8] to be

$$|V_{us}| = \lambda = 0.2196 \pm 0.0023 . \tag{4}$$

  In our fits, we ignore the small error on λ.

- $|V_{cb}|$: The determination of $|V_{cb}|$ from inclusive and exclusive B decays has been studied in a number of papers [9, 10, 11, 12, 13]. The number used here is taken from the Particle Data Group compilation [8]:

$$|V_{cb}| = 0.0395 \pm 0.0017 , \tag{5}$$

  yielding

$$A = 0.819 \pm 0.035 . \tag{6}$$

- $|V_{ub}/V_{cb}|$: The knowledge of the CKM matrix element ratio $|V_{ub}/V_{cb}|$ is based on the analysis of the end-point lepton energy spectrum in semileptonic decays $B \to X_u \ell \nu_\ell$ and the measurement of the exclusive semileptonic decays $B \to (\pi, \rho) \ell \nu_\ell$. Present measurements in both the inclusive and exclusive modes are compatible with [12]:

$$\left| \frac{V_{ub}}{V_{cb}} \right| = 0.093 \pm 0.014 . \tag{7}$$

  This gives

$$\sqrt{\rho^2 + \eta^2} = 0.423 \pm 0.064 . \tag{8}$$

- $|\epsilon|, \hat{B}_K$: The experimental value of $|\epsilon|$ is [8]:

$$|\epsilon| = (2.280 \pm 0.013) \times 10^{-3} . \tag{9}$$

  In the standard model, $|\epsilon|$ is essentially proportional to the imaginary part of the box diagram for K^0–$\overline{K^0}$ mixing and is given by [14]

$$|\epsilon| = \frac{G_F^2 f_K^2 M_K M_W^2}{6\sqrt{2}\pi^2 \Delta M_K} \hat{B}_K \left(A^2 \lambda^6 \eta \right) (y_c \{ \hat{\eta}_{ct} f_3(y_c, y_t) - \hat{\eta}_{cc} \}$$
$$+ \hat{\eta}_{tt} y_t f_2(y_t) A^2 \lambda^4 (1 - \rho)), \tag{10}$$

  where $y_i \equiv m_i^2/M_W^2$, and the functions f_2 and f_3 are:

$$f_2(x) = \frac{1}{4} + \frac{9}{4}\frac{1}{(1-x)} - \frac{3}{2}\frac{1}{(1-x)^2} - \frac{3}{2}\frac{x^2 \ln x}{(1-x)^3} ,$$
$$f_3(x, y) = \ln \frac{x}{y} - \frac{3y}{4(1-y)}\left(1 + \frac{y}{1-y} \ln y \right) . \tag{11}$$

4

(The above form for $f_3(x, y)$ is an approximation, obtained in the limit $x \ll y$. For the exact expression, see Ref. [15].) Here, the $\hat{\eta}_i$ are QCD correction factors, calculated at next-to-leading order in Refs. [16] ($\hat{\eta}_{cc}$), [17] ($\hat{\eta}_{tt}$) and [18] ($\hat{\eta}_{ct}$). The theoretical uncertainty in the expression for $|\epsilon|$ is in the renormalization-scale independent parameter $\hat{B}_K$, which represents our ignorance of the hadronic matrix element $\langle K^0|(\overline{d}\gamma^\mu(1 - \gamma_5)s)^2|\overline{K^0}\rangle$. Recent calculations of $\hat{B}_K$ using lattice QCD methods are summarized in Refs. [19, 20], yielding

$$\hat{B}_K = 0.94 \pm 0.15. \tag{12}$$

- $\Delta M_d, f_{B_d}^2 \hat{B}_{B_d}$: The present world average for ΔM_d is [21]

$$\Delta M_d = 0.471 \pm 0.016 \ (ps)^{-1} \ . \tag{13}$$

The mass difference ΔM_d is calculated from the B_d^0–$\overline{B_d^0}$ box diagram. Unlike the kaon system, where the contributions of both the c- and the t-quarks in the loop are important, this diagram is dominated by t-quark exchange:

$$\Delta M_d = \frac{G_F^2}{6\pi^2} M_W^2 M_B \left(f_{B_d}^2 \hat{B}_{B_d}\right) \hat{\eta}_B y_t f_2(y_t) |V_{td}^* V_{tb}|^2 \ , \tag{14}$$

where, using Eq. (1), $|V_{td}^* V_{tb}|^2 = A^2 \lambda^6 [(1 - \rho)^2 + \eta^2]$. Here, $\hat{\eta}_B$ is the QCD correction. In the fits presented in Ref. [22] we used the value $\hat{\eta}_B = 0.55$, calculated in the $\overline{MS}$ scheme, following Ref. [17]. Consistency requires that the top quark mass be rescaled from its pole (mass) value of $m_t = 175 \pm 5$ GeV to the value $\overline{m_t}(m_t(pole)) = 165 \pm 5$ GeV in the $\overline{MS}$ scheme. We shall ignore the slight dependence of $\hat{\eta}_B$ on $\overline{m_t}(m_t(pole))$ in the range given here.

For the B system, the hadronic uncertainty is given by $f_{B_d}^2 \hat{B}_{B_d}$, analogous to $\hat{B}_K$ in the kaon system, except that in this case f_{B_d} has not been measured. Present estimates of this quantity are summarized in Refs. [19, 20], yielding $f_{B_d}\sqrt{\hat{B}_{B_d}} = (190 \pm 23)$ MeV in the quenched approximation. The effect of unquenching is not yet understood completely. Taking the MILC collaboration estimates of unquenching would increase the central value of $f_{B_d}\sqrt{\hat{B}_{B_d}}$ by 21 MeV [23]. In our fits, we have taken

$$f_{B_d}\sqrt{\hat{B}_{B_d}} = 215 \pm 40 \ \text{MeV} \ , \tag{15}$$

which is a fairly conservative estimate of the present theoretical error on this quantity.

- $\Delta M_s, f_{B_s}^2 \hat{B}_{B_s}$: Mixing in the B_s^0–$\overline{B_s^0}$ system is quite similar to that in the B_d^0–$\overline{B_d^0}$ system. The B_s^0–$\overline{B_s^0}$ box diagram is again dominated by t-quark exchange, and the mass difference between the mass eigenstates ΔM_s is given by a formula analogous to that of Eq. (14):

$$\Delta M_s = \frac{G_F^2}{6\pi^2} M_W^2 M_{B_s} \left(f_{B_s}^2 \hat{B}_{B_s}\right) \hat{\eta}_{B_s} y_t f_2(y_t) |V_{ts}^* V_{tb}|^2 \ . \tag{16}$$

Using the fact that $|V_{cb}| = |V_{ts}|$ (Eq. (1)), it is clear that one of the sides of the unitarity triangle, $|V_{td}/\lambda V_{cb}|$, can be obtained from the ratio of ΔM_d and ΔM_s,

$$\frac{\Delta M_s}{\Delta M_d} = \frac{\hat{\eta}_{B_s} M_{B_s} \left(f_{B_s}^2 \hat{B}_{B_s}\right)}{\hat{\eta}_{B_d} M_{B_d} \left(f_{B_d}^2 \hat{B}_{B_d}\right)} \left|\frac{V_{ts}}{V_{td}}\right|^2 \ . \tag{17}$$

5

The only real uncertainty in this quantity is the ratio of hadronic matrix elements $f_{B_s}^2 \hat{B}_{B_s} / f_{B_d}^2 \hat{B}_{B_d}$. It is now widely accepted that the ratio $\xi_s \equiv (f_{B_s} \sqrt{\hat{B}_{B_s}}) / (f_{B_d} \sqrt{\hat{B}_{B_d}})$ is probably the most reliable of the lattice-QCD estimates in B physics, and the present estimate is [19, 20]:

$$\xi_s = 1.14 \pm 0.06 . \tag{18}$$

The present lower bound on ΔM_s is: $\Delta M_s > 12.4$ (ps)$^{-1}$ (at 95% C.L.) [12]. This bound has been established using the so-called "amplitude method" [24]. This method is also the best procedure for including information about B_s^0–$\overline{B_s^0}$ mixing in the fit, and works as follows. Given a meson which at $t = 0$ was pure B_s^0, the probability for it to be detected as a B_s^0 at time t is

$$P = \frac{1}{2\tau} e^{-t/\tau} \left(1 + \cos \Delta M_s t \right), \tag{19}$$

while the probability for it to be detected as a $\overline{B_s^0}$ is

$$P = \frac{1}{2\tau} e^{-t/\tau} \left(1 - \cos \Delta M_s t \right). \tag{20}$$

In the amplitude method, one introduces the amplitude $\mathcal{A}$ and writes the oscillations terms as $(1 \pm \mathcal{A} \cos \Delta M_s t)$. One then measures the value of $\mathcal{A}$, along with its error $\sigma_{\mathcal{A}}$ assuming various values of ΔM_s. For a given value of ΔM_s, if $\mathcal{A}$ is compatible with 0, one concludes that there is no visible oscillation at this frequency; if $\mathcal{A}$ is compatible with 1, one concludes that an oscillation was observed at this frequency.

The experimental data consists of measured values of $\mathcal{A}$ and $\sigma_{\mathcal{A}}$ for various values of ΔM_s. To include this data in the fit, for each set of free parameters (A, ρ, η, ξ_s) we calculate the value of ΔM_s and find the corresponding experimental values of $\mathcal{A}$ and $\sigma_{\mathcal{A}}$. Since a nonzero value of ΔM_s implies that there is B_s^0–$\overline{B_s^0}$ mixing, theoretically one should have $\mathcal{A} = 1$. For this set of parameters we therefore add to the global χ^2 a factor

$$\left(\frac{\mathcal{A} - 1}{\sigma_{\mathcal{A}}} \right)^2 . \tag{21}$$

(There is also a similar factor which takes into account the deviation of ξ_s from its central value (Eq. (18)).)

The data used in our fits are summarized in Table 1. The quantities with the largest errors are $\hat{\eta}_{cc}$ (28%), $\hat{B}_K$ (16%), $|V_{ub}/V_{cb}|$ (15%) and $f_{B_d} \sqrt{\hat{B}_{B_d}}$ (19%). Of these, the latter three are extremely important in defining the allowed ρ–η region (the large error on $\hat{\eta}_{cc}$ does not affect the fit very much). The errors on two of these quantities — $\hat{B}_K$ and $f_{B_d} \sqrt{\hat{B}_{B_d}}$ — are purely theoretical in origin, and the error on $|V_{ub}/V_{cb}|$ has a significant theoretical component (model dependence). Thus, the present uncertainty in the shape of the unitarity triangle is due in large part to theoretical errors. Reducing these errors will be quite important in getting a precise profile of the unitarity triangle and the CP-violating phases.

There are two other measurements which should be mentioned here.

Parameter	Value
λ	0.2196
$|V_{cb}|$	0.0395 ± 0.0017
$|V_{ub}/V_{cb}|$	0.093 ± 0.014
$|\epsilon|$	$(2.280 \pm 0.013) \times 10^{-3}$
ΔM_d	$(0.471 \pm 0.016)\ (ps)^{-1}$
ΔM_s	$> 12.4\ (ps)^{-1}$
$\overline{m_t}(m_t(pole))$	(165 ± 5) GeV
$\overline{m_c}(m_c(pole))$	1.25 ± 0.05 GeV
$\hat{\eta}_B$	0.55
$\hat{\eta}_{cc}$	1.38 ± 0.53
$\hat{\eta}_{ct}$	0.47 ± 0.04
$\hat{\eta}_{tt}$	0.57
$\hat{B}_K$	0.94 ± 0.15
$f_{B_d}\sqrt{\hat{B}_{B_d}}$	215 ± 40 MeV
ξ_s	1.14 ± 0.06

Table 1: Data used in the CKM fits. Values of the hadronic quantities $\hat{B}_K$, $f_{B_d}\sqrt{\hat{B}_{B_d}}$, and ξ_s are taken from the lattice QCD results [19, 20]. The remaining theoretical numbers are discussed in the text. The value for ΔM_d and the 95% C.L. lower limit on ΔM_s are taken from the LEP Electroweak group [12]. All other experimental numbers are taken from the Particle Data Group [8].

First, the KTEV collaboration [25] has recently reported a measurement of direct CP violation in the K sector through the ratio ϵ'/ϵ, with

$$\text{Re}(\epsilon'/\epsilon) = (28.0 \pm 3.0(\text{stat}) \pm 2.6(\text{syst}) \pm 1.0(\text{MC stat})) \times 10^{-4} \, , \tag{22}$$

in agreement with the earlier measurement by the CERN experiment NA31 [26], which reported a value of $(23 \pm 6.5) \times 10^{-4}$ for the same quantity. The present world average is $\text{Re}(\epsilon'/\epsilon) = (21.8 \pm 3.0) \times 10^{-4}$. This combined result excludes the superweak model [27] by more than 7σ.

A great deal of theoretical effort has gone into calculating this quantity at next-to-leading order accuracy in the SM [28, 29, 30]. The result of this calculation has been summarized in a succint form by Buras and Silvestrini [31]:

$$\text{Re}(\epsilon'/\epsilon) = \text{Im}\lambda_t \left[-1.35 + R_s \left(1.1 |r_Z^{(8)}| B_6^{(1/2)} + (1.0 - 0.67 |r_Z^{(8)}|) B_8^{(3/2)} \right) \right] \, . \tag{23}$$

Here $\lambda_t = V_{td} V_{ts}^* = A^2 \lambda^4 \eta$ and $r_Z^{(8)}$ represents the short-distance contribution, which at the NLO precision is estimated to lie in the range $6.5 \leq |r_Z^{(8)}| \leq 8.5$ [28, 29]. The quantities $B_6^{(1/2)} = B_6^{(1/2)}(m_c)$ and $B_8^{(3/2)} = B_8^{(3/2)}(m_c)$ are the matrix elements of the $\Delta I = 1/2$ and $\Delta I = 3/2$ operators O_6 and O_8, respectively, calculated at the scale $\mu = m_c$. Lattice-QCD [32] and the $1/N_c$ expansion [33] yield:

$$0.8 \leq B_6^{(1/2)} \leq 1.3, \qquad 0.6 \leq B_8^{(3/2)} \leq 1.0 \, . \tag{24}$$

Finally, the quantity R_s in Eq. (23) is defined as:

$$R_s \equiv \left(\frac{150 \text{ MeV}}{m_s(m_c) + m_d(m_c)} \right)^2 \, , \tag{25}$$

essentially reflecting the s-quark mass dependence. The present uncertainty on the CKM matrix element is $\pm 23\%$, which is already substantial. However, the theoretical uncertainties related to the other quantities discussed above are considerably larger. For example, the ranges $\epsilon'/\epsilon = (5.3 \pm 3.8) \times 10^{-4}$ and $\epsilon'/\epsilon = (8.5 \pm 5.9) \times 10^{-4}$, assuming $m_s(m_c) = 150 \pm 20$ MeV and $m_s(m_c) = 125 \pm 20$ MeV, respectively, have been quoted as the best representation of the status of ϵ'/ϵ in the SM [34]. These estimates are somewhat on the lower side compared to the data but not inconsistent. (For some recent speculations on new physics, see Refs. [35, 36].)

Thus, whereas ϵ'/ϵ represents a landmark measurement, removing the superweak model of Wolfenstein and its kith and kin from further consideration, its impact on CKM phenomenology, particularly in constraining the CKM parameters, is marginal. Probably the best use of this measurement is to constrain the s-quark mass, which at present has considerable uncertainty. For this reason we do not include the measurement of ϵ'/ϵ in the CKM fits presented here.

Second, the CDF collaboration has recently made a measurement of $\sin 2\beta$ [37]. In the Wolfenstein parametrization, $-\beta$ is the phase of the CKM matrix element V_{td}. From Eq. (1) one can readily find that

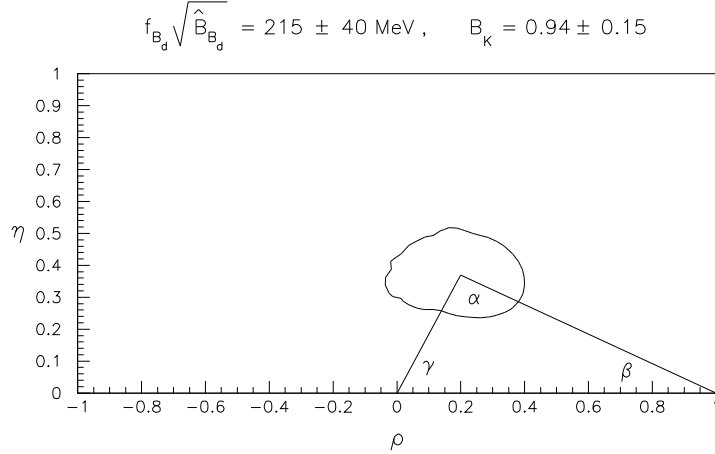$$\sin(2\beta) = \frac{2\eta(1 - \rho)}{(1 - \rho)^2 + \eta^2} \, . \tag{26}$$

$f_{B_d}\sqrt{\hat{B}_{B_d}} = 215 \pm 40 \text{ MeV}, \qquad B_K = 0.94 \pm 0.15$

Figure 2: Allowed region in ρ–η space in the SM, from a fit to the ten parameters discussed in the text and given in Table 1. The limit on ΔM_s is included using the amplitde method of Ref. [24]. The theoretical errors on $f_{B_d}\sqrt{\hat{B}_{B_d}}$, $\hat{B}_K$ and ξ_s are treated as Gaussian. The solid line represents the region with $\chi^2 = \chi^2_{min} + 6$ corresponding to the 95% C.L. region. The triangle shows the best fit.

Thus, a measurement of $\sin 2\beta$ would put a strong contraint on the parameters ρ and η. However, the CDF measurement gives [37]

$$\sin 2\beta = 0.79^{+0.41}_{-0.44} \ , \tag{27}$$

or $\sin 2\beta > 0$ at 93% C.L. As we will see in the next section, this constraint is quite weak – the other measurements already constrain $0.52 \leq \sin 2\beta \leq 0.94$ at the 95% C.L. in the SM. (The CKM fits reported in Refs. [12, 13, 38] yield similar ranges.) In light of this, and given that it is not clear how to combine the above measurement (which allows for unphysical values of $\sin 2\beta$) with the other data, we have not included this measurement in our fits.

2.2 SM Fits

In order to find the allowed region in ρ–η space, i.e. the allowed shapes of the unitarity triangle, the computer program MINUIT is used to fit the parameters to the constraints described above. In the fit, we allow ten parameters to vary: ρ, η, A, m_t, m_c, η_{cc}, η_{ct}, $f_{B_d}\sqrt{\hat{B}_{B_d}}$, $\hat{B}_K$, and ξ_s. The ΔM_s constraint is included using the amplitude method.

The allowed (95% C.L.) ρ–η region is shown in Fig. 2. The best fit has $(\rho, \eta) = (0.20, 0.37)$.

There is an alternative way to include the ΔM_s constraint, one which we have used in the past [22]. In this case the constraint is excluded from the fit, but rather one cuts away a region of ρ–η space by superimposing a line corresponding to a particular value of ξ_s. Using the 95% C.L. limit on ΔM_s and allowing ΔM_d to fluctuate upward by 1σ from its central value, one obtains $\Delta M_s/\Delta M_d > 25.5$. This yields the following constraint on ρ and η:

$$\lambda^2 \left[(1-\rho)^2 + \eta^2 \right] = \left(\frac{\Delta M_d}{\Delta M_s} \right) \xi_s^2 \leq \frac{1}{25.5} (1.14 \pm 0.06)^2 \ . \tag{28}$$
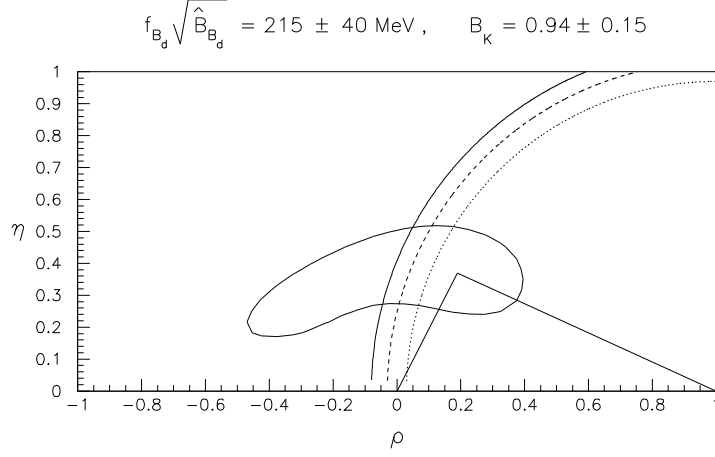
9

$$f_{B_d}\sqrt{\hat{B}_{B_d}} = 215 \pm 40 \text{ MeV}, \qquad B_K = 0.94 \pm 0.15$$

Figure 3: Allowed region in ρ–η space in the SM. The ΔM_s limit is not included in the fit, but rather imposed by cutting away a region of the space. The disallowed region is shown for three choices of the parameter ξ_s: 1.08 (dotted line), 1.14 (dashed line), 1.20 (solid line). In all cases, the region to the left of the curve is ruled out.

We take three candidate values for ξ_s: 1.08, 1.14, 1.20. The results are shown in Fig. 3. The best fit has $(\rho, \eta) = (0.19, 0.37)$.

A comparison of Figs. 2 and 3 reveals that the allowed regions are similar, though not identical, for the two methods of including the ΔM_s constraint. Henceforth, all our results will be presented using the fit which includes this constraint via the amplitude method.

The CP angles α, β and γ can be measured in CP-violating rate asymmetries in B decays [3]. For example, the asymmetries in $B_d^0(t) \to \pi^+\pi^-$ and $B_d^0(t) \to J/\Psi K_s$ probe $\sin 2\alpha$ and $\sin 2\beta$, respectively. The angle γ can be extracted from $B^\pm \to DK^\pm$ [39] or $B_s^0(t) \to D_s^\pm K^\mp$ [40]. The function in this case is $\sin^2 \gamma$.

From Fig. 1, it is clear that these angles can be expressed in terms of ρ and η. Thus, different shapes of the unitarity triangle are equivalent to different values of the CP angles. Referring to Fig. 2, we note that the preferred (central) values of these angles are $(\alpha, \beta, \gamma) = (93°, 25°, 62°)$. The allowed ranges at 95% C.L. are

$$
\begin{aligned}
65° &\leq \alpha \leq 123° \\
16° &\leq \beta \leq 35° \\
36° &\leq \gamma \leq 97°
\end{aligned}
\tag{29}
$$

or, equivalently,

$$
\begin{aligned}
-0.91 &\leq \sin 2\alpha \leq 0.77 \\
0.52 &\leq \sin 2\beta \leq 0.94 \\
0.35 &\leq \sin^2 \gamma \leq 1.00 \ .
\end{aligned}
\tag{30}
$$

Of course, the values of α, β and γ are correlated, i.e. they are not all allowed simultaneously. After all, the sum of these angles must equal 180°. We illustrate these correlations in Figs. 4
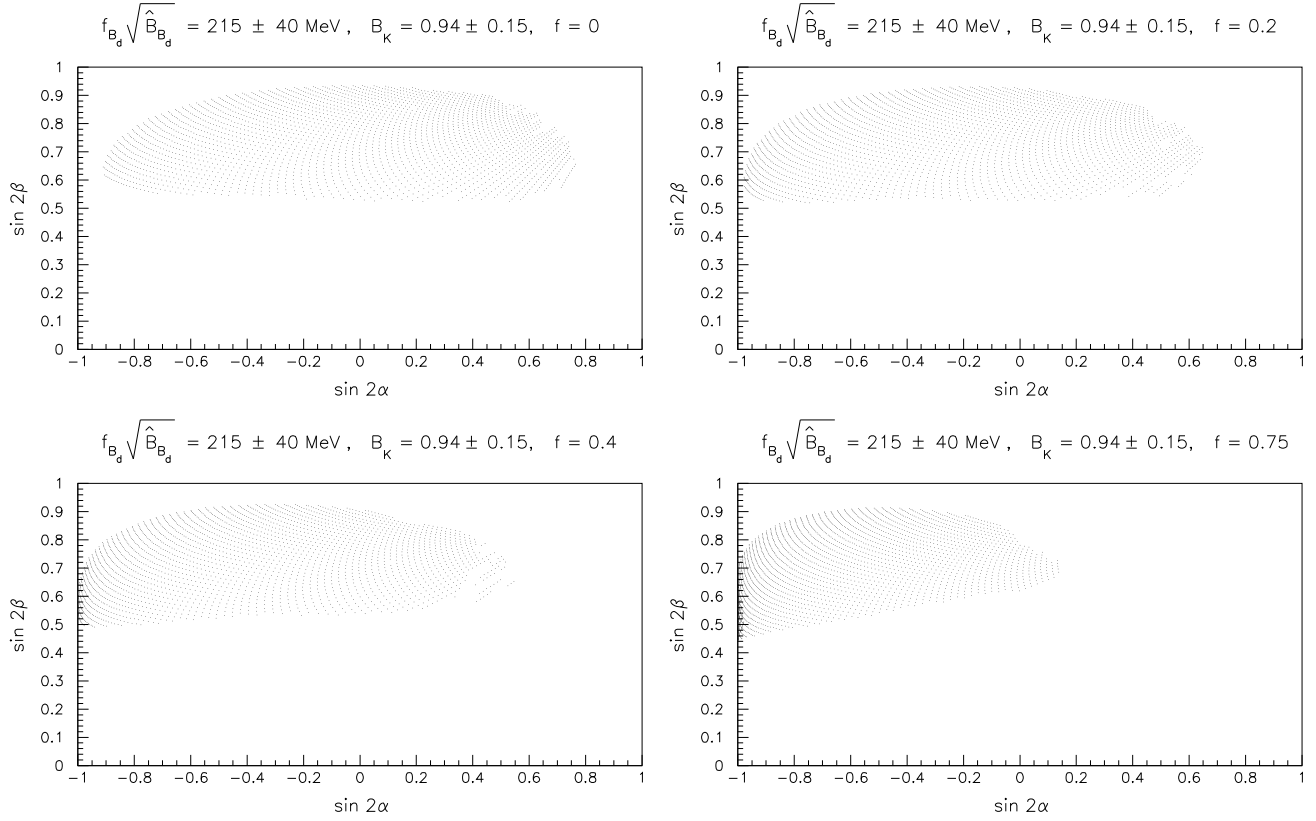
Figure 4: Allowed 95% C.L. region of the CP-violating quantities $\sin 2\alpha$ and $\sin 2\beta$, from a fit to the data given in Table 1. The upper left plot ($f = 0$) corresponds to the SM, while the other plots ($f = 0.2$, 0.4, 0.75) correspond to various SUSY models.

and 5. The plots with $f = 0$ correspond to the SM. (Nonzero values of f correspond to supersymmetric models, which will be discussed in detail in the next section.) Fig. 4 shows the allowed region in $\sin 2\alpha$–$\sin 2\beta$ space allowed by the data. And Fig. 5 shows the allowed (correlated) values of the CP angles α and γ. This correlation is roughly linear, due to the relatively small allowed range of β (Eq. (29)).

3   Unitarity Triangle: A SUSY Profile

In this section we examine the profile of the unitarity triangle in supersymmetric (SUSY) theories. As we will see below, the most general models contain a number of unconstrained phases and so are not sufficiently predictive to perform such an analysis. However, there is a class of SUSY models in which these phases are constrained to be approximately zero, which greatly increases the predictivity. Not surprisingly, the calculations of the SUSY contributions to measured quantities are also more advanced in these models, having been performed at the next-to-leading-order (NLO) level. In the following subsections, we discuss aspects of more
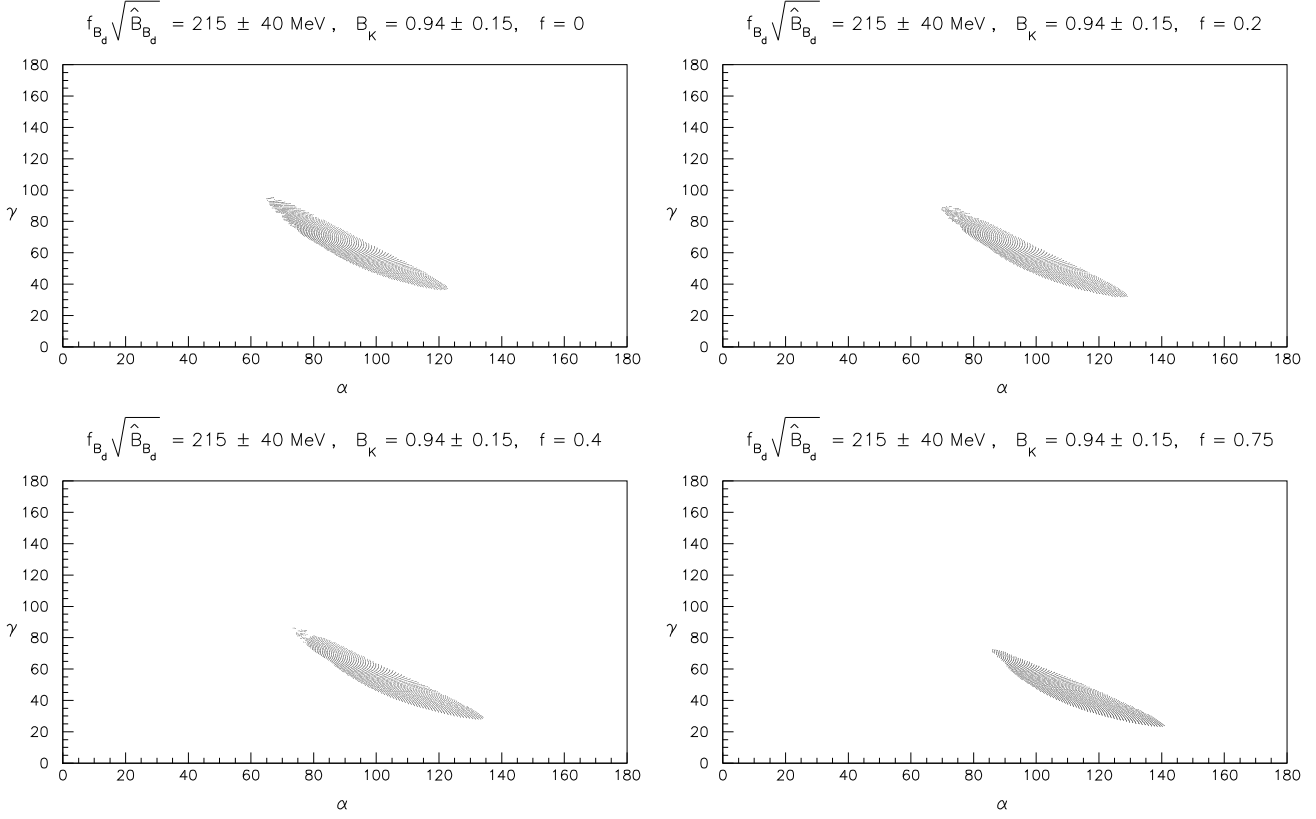
11

Figure 5: Allowed 95% C.L. region of the CP-violating quantities α and γ, from a fit to the data given in Table 1. The upper left plot ($f = 0$) corresponds to the SM, while the other plots ($f = 0.2, 0.4, 0.75$) correspond to various SUSY models.

general SUSY theories, as well as the details of that class of theories whose effects on the unitarity triangle can be directly analyzed.

3.1 Flavour Violation in SUSY Models - Overview

We begin with a brief review of flavour violation in the minimal supersymmetric standard model (MSSM).

The low energy effective theory in the MSSM can be specified in terms of the chiral superfields for the three generations of quarks (Q_i, U_i^c, and D_i^c) and leptons (L_i and E_i^c), chiral superfields for two Higgs doublets (H_1 and H_2), and vector superfields for the gauge group $SU(3)_C \times SU(2)_I \times U(1)_Y$ [41]. The superpotential is given by

$$W_{MSSM} = f_D^{ij} Q_i D_j H_1 + f_U^{ij} Q_i U_j H_2 + f_L^{ij} E_i L_j H_1 + \mu H_1 H_2. \tag{31}$$

The indices $i, j = 1, 2, 3$ are generation indices and f_D^{ij}, f_U^{ij}, f_L^{ij} are Yukawa coupling matrices in the generation space. A general form of the soft SUSY-breaking term is given by

$$
\begin{aligned}
-\mathcal{L}_{\text{soft}} = {}& (m_Q^2)_j^i \tilde{q}_i \tilde{q}^{\dagger j} + (m_D^2)_j^i \tilde{d}_i \tilde{d}^{\dagger j} + (m_U^2)_j^i \tilde{u}_i \tilde{u}^{\dagger j} + (m_E^2)_j^i \tilde{e}_i \tilde{e}^{\dagger j} + (m_L^2)_j^i \tilde{\ell}_i \tilde{\ell}^{\dagger j} \\
& + \Delta_1^2 h_1^\dagger h_1 + \Delta_2^2 h_2^\dagger h_2 - (B\mu h_1 h_2 + h.c.) \\
& + (A_D^{ij} \tilde{q}_i \tilde{d}_j h_1 + A_U^{ij} \tilde{q}_i \tilde{u}_j h_2 + A_L^{ij} \tilde{e}_i \tilde{\ell}_j h_1 + h.c.) \\
& + (\frac{M_1}{2} \tilde{B}\tilde{B} + \frac{M_2}{2} \tilde{W}\tilde{W} + \frac{M_3}{2} \tilde{G}\tilde{G} + h.c.),
\end{aligned}
\tag{32}
$$

where $\tilde{q}_i$, $\tilde{u}_i$, $\tilde{d}_i$, $\tilde{\ell}_i$, $\tilde{e}_i$, h_1 and h_2 are scalar components of the superfields Q_i, U_i, D_i, L_i, E_i, H_1 and H_2, respectively, and $\tilde{B}$, $\tilde{W}$ and $\tilde{G}$ are the $U(1)$, $SU(2)$ and $SU(3)$ gauge fermions, respectively.

In fact, there are many variants of the MSSM. All have the same particle content, but the mass hierarchies and supersymmetry-breaking parameters are different. As a result, they lead to different low-energy predictions.

For example, in supergravity (SUGRA) models, the SUSY-breaking parameters in the MSSM are assumed to have a simple structure at the Planck scale [41]. Neglecting the difference between the Planck and the GUT scales, and defining this scale by X, one can express them as follows:

$$
\begin{aligned}
(m_Q^2)_j^i &= (m_E^2)_j^i = m_0^2 \delta_j^i, \\
(m_D^2)_j^i &= (m_U^2)_j^i = (m_L^2)_j^i = m_0^2 \delta_j^i, \\
\Delta_1^2 &= \Delta_2^2 = \Delta_0^2, \\
A_D^{ij} &= f_{DX}^{ij} A_X m_0, \quad A_L^{ij} = f_{LX}^{ij} A_X m_0, \quad A_U^{ij} = f_{UX}^{ij} A_X m_0, \\
M_1 &= M_2 = M_3 = M_{gX} \ .
\end{aligned}
\tag{33}
$$

In the minimal SUGRA case, $m_0 = \Delta_0$, while in the non-minimal SUGRA case, one takes m_0 and Δ_0 as independent parameters.

13

In general, MSSM models have three physical phases, apart from the QCD vacuum parameter $\bar{\theta}_{QCD}$ which we shall take to be zero. The three phases are: (i) the CKM phase represented here by the Wolfenstein parameter η, (ii) the phase $\theta_A = \arg(A)$, and (iii) the phase $\theta_\mu = \arg(\mu)$ [42]. The last two phases are peculiar to SUSY models and their effects must be taken into account in a general supersymmetric framework. In particular, the CP-violating asymmetries which result from the interference between mixing and decay amplitudes can produce non-standard effects. Concentrating here on the $\Delta B = 2$ amplitudes, two new phases θ_d and θ_s arise, which can be parametrized as follows [43]:

$$\theta_{d,s} = \frac{1}{2} \arg \left(\frac{\langle B_{d,s} | \mathcal{H}_{eff}^{SUSY} | \bar{B}_{d,s} \rangle}{\langle B_{d,s} | \mathcal{H}_{eff}^{SM} | \bar{B}_{d,s} \rangle} \right) \ , \tag{34}$$

where $\mathcal{H}^{SUSY}$ is the effective Hamiltonian including both the SM degrees of freedom and the SUSY contributions. Thus, CP-violating asymmetries in B decays would involve not only the phases α, β and γ, defined previously, but additionally θ_d or θ_s. In other words, the SUSY contributions to the real parts of $M_{12}(B_d)$ and $M_{12}(B_s)$ are *no longer proportional* to the CKM matrix elements $V_{td} V_{tb}^*$ and $V_{ts} V_{tb}^*$, respectively. If θ_d or θ_s were unconstrained, one could not make firm predictions about the CP asymmetries in SUSY models. In this case, an analysis of the profile of the unitarity triangle in such models would be futile.

However, the experimental upper limits on the electric dipole moments (EDM) of the neutron and electron [8] do provide constraints on the phases θ_μ and θ_A [44]. In SUGRA models with *a priori* complex parameters A and μ, the phase θ_μ is strongly bounded with $\theta_\mu < 0.01\pi$ [45]. The phase θ_A can be of $O(1)$ in the small θ_μ region, as far as the EDMs are concerned. In both the $\Delta S = 2$ and $\Delta B = 2$ transitions, and for low-to-moderate values of $\tan \upsilon$ [1], it has been shown that θ_A does not change the phase of either the matrix element $M_{12}(K)$ [42] or of $M_{12}(B)$ [45]. Hence, in SUGRA models, $\arg M_{12}(B)|_{SUGRA} = \arg M_{12}(B)|_{SM} = \arg(\xi_t^2)$, where $\xi_t = V_{td}^* V_{tb}$. Likewise, the phase of the SUSY contribution in $M_{12}(K)$ is aligned with the phase of the $t\bar{t}$-contribution in $M_{12}(K)$, given by $\arg(V_{td} V_{ts}^*)$. Thus, in SUGRA models, one can effectively set $\theta_d \simeq 0$ and $\theta_s \simeq 0$, so that the CP-violating asymmetries give information about the SM phases α, β and γ. Hence, an analysis of the UT and CP-violating phases α, β and γ can be carried out in a very similar fashion as in the SM, taking into account the additional contributions to $M_{12}(K)$ and $M_{12}(B)$.

For large-$\tan \upsilon$ solutions, one has to extend the basis of $H_{eff}(\Delta B = 2)$ so as to include new operators whose contribution is small in the low-$\tan \upsilon$ limit. The resulting effective Hamiltonian is given by

$$H_{eff}(\Delta B = 2) = \frac{G_F^2 M_W^2}{2\pi^2} \sum_{i=1}^{3} C_i(\mu) O_i \ , \tag{35}$$

where $O_1 = \bar{d}_L^\alpha \gamma_\mu b_L^\alpha \bar{d}_L^\beta \gamma^\mu b_L^\beta$, $O_2 = \bar{d}_L^\alpha b_R^\alpha \bar{d}_L^\beta b_R^\beta$ and $O_3 = \bar{d}_L^\alpha b_R^\beta \bar{d}_L^\beta b_R^\alpha$ and C_i are the Wilson coefficients [46, 47]. The coefficients $C_1(\mu)$ and $C_2(\mu)$ are real relative to the SM contribution.

---

[1] In supersymmetric jargon, the quantity $\tan \beta$ is used to define the ratio of the two vacuum expectation values (vevs) $\tan \beta \equiv v_u/v_d$, where $v_d(v_u)$ is the vev of the Higgs field which couples exclusively to down-type (up-type) quarks and leptons. (See, for example, the review by Haber in Ref. [8]). However, in discussing flavour physics, the symbol β is traditionally reserved for one of the angles of the unitarity triangle. To avoid confusion, we will call the ratio of the vevs $\tan \upsilon$.

However, the chargino contributions to $C_3(\mu)$ are generally complex relative to the SM contribution and can generate a new phase shift in the B^0–$\overline{B^0}$ mixing amplitude [48, 49]. This effect is in fact significant for large $\tan v$ [46], since $C_3(\mu)$ is proportional to $(m_b/m_W \cos\beta)^2$. How large this additional phase (θ_d and θ_s) can be depends on how the constraints from EDM are imposed. For example, Baek and Ko [49] find that in the MSSM without imposing the EDM constraint, one has $2|\theta_d| \leq 6°$ for a light stop and large $\tan v$ but this phase becomes practically zero if the EDM constraints [50] are imposed. This aspect of the analysis in Ref. [49], though done without invoking the SUGRA model mass relations, should also hold in SUGRA models.

In a more general supersymmetric scenario, the SUSY effects may lead to additional phases and the constraints from EDMs may not be sufficient to effectively bound them. (A recent example is the so-called "effective supersymmetry" [43].) As discussed above, such models do not make clean predictions for the CP asymmetries, so that one cannot analyse the profile of the unitarity triangle in this case. Instead, flavour-changing effects in K and B decays in these scenarios will have to be disentangled along the lines suggested in Refs. [43, 51, 52]. These theories may give rise to flavour-violation effects which are uncharacteristic of the SM and MSSM. In particular, they may lead to a measurable charge asymmetry in semileptonic decays of the B^0 and $\overline{B^0}$ [52], which is estimated to be negligible in both the SM and MSSM/SUGRA models discussed above. However, some technical aspects in the most general supersymmetric theories remain to be worked out. For example, the complete NLO corrections for ΔM_d, ΔM_s and $|\epsilon|$ have not been calculated in these theories. The bag constants which correct for the vacuum insertion approximation in the matrix elements of the operators in $H_{eff}^{\Delta S=2}$ have been calculated using lattice-QCD techniques [53], but the corresponding estimates for the bag parameters $H_{eff}^{\Delta B=2}$ are not yet available. Likewise, the NLO calculations in the general supersymmetric case for the decay $B \to X_s \gamma$ are not yet at hand. This last ingredient enters the estimates of the quantities ΔM_d, ΔM_s and $|\epsilon|$ indirectly as the measured branching ratio $\mathcal{B}(B \to X_s \gamma)$ provides rather stringent constraints on the allowed supersymmetric parameters.

In view of the foregoing, we shall restrict ourselves to a class of SUSY models in which the following features, related to flavour mixing, hold:

- The squark flavour mixing matrix which diagonalizes the squark mass matrix is approximately the same as the corresponding quark mixing matrix V_{CKM}, apart from the left-right mixing of the top squarks.

- The first- and second-generation squarks with the same gauge quantum numbers remain highly degenerate in masses but the third-generation squarks, especially the top squark, can be significantly lighter due to the renormalization effect of the top Yukawa coupling constants.

- The phases θ_d and θ_s are negligible in the entire $\tan v$ plane, once the constraints from the EDMs of neutron and lepton are consistently imposed.

These features lead to an enormous simplification in the flavour structure of the SUSY contributions to flavour-changing processes. In particular, SUSY contributions to the transitions $b \to s$, $b \to d$ and $s \to d$ are proportional to the CKM factors, $V_{tb}V_{ts}^*$, $V_{tb}V_{td}^*$ and $V_{ts}V_{td}^*$, respectively. Similarly, the SUSY contributions to the mass differences $M_{12}(B_s)$, $M_{12}(B_d)$ and

$M_{12}(K)$ are proportional to the CKM factors $(V_{tb}V_{ts}^*)^2$, $(V_{tb}V_{td}^*)^2$ and $(V_{ts}V_{td}^*)^2$, respectively. These are precisely the same factors which govern the contribution of the top quark in these transitions in the standard model. Thus, the supersymmetric contributions can be implemented in a straightforward way by adding a (supersymmetric) piece in each of the above mentioned amplitudes to the corresponding top quark contribution in the SM.

3.2 NLO Corrections to ΔM_d, ΔM_s and ϵ in Minimal SUSY Flavour Violation

A number of SUSY models share the features mentioned in the previous subsection, and the supersymmetric contributions to the mass differences $M_{12}(B)$ and $M_{12}(K)$ have been analyzed in a number of papers [45, 46, 54, 55, 56, 57], following the pioneering work of Ref. [58]. Following these papers, ΔM_d can be expressed as:

$$\Delta M_d = \frac{G_F^2}{6\pi^2} M_W^2 M_B \left(f_{B_d}^2 \hat{B}_{B_d} \right) \hat{\eta}_B \left[A_{SM}(B) + A_{H^\pm}(B) + A_{\chi^\pm}(B) + A_{\tilde{g}}(B) \right] , \qquad (36)$$

where the function $A_{SM}(B)$ can be written by inspection from Eq. (14):

$$A_{SM}(B) = y_t f_2(y_t) |V_{td}^* V_{tb}|^2 . \qquad (37)$$

The expressions for $A_{H^\pm}(B)$, $A_{\chi^\pm}(B)$ and $A_{\tilde{g}}(B)$ are obtained from the SUSY box diagrams. Here, $H^\pm$, $\chi_j^\pm$, $\tilde{t}_a$ and $\tilde{d}_i$ represent, respectively, the charged Higgs, chargino, stop and down-type squarks. The contribution of the intermediate states involving neutralinos is small and usually neglected. The expressions for $A_{H^\pm}(B)$, $A_{\chi^\pm}(B)$ and $A_{\tilde{g}}(B)$ are given explicitly in the literature [46, 54, 58].

We shall not be using the measured value of the mass difference ΔM_K due to the uncertain contribution of the long-distance contribution. However, $|\epsilon|$ is a short-distance dominated quantity and in supersymmetric theories can be expressed as follows:

$$|\epsilon| = \frac{G_F^2 f_K^2 M_K M_W^2}{6\sqrt{2}\pi^2 \Delta M_K} \hat{B}_K \left[\text{Im } A_{SM}(K) + \text{Im } A_{H^\pm}(K) + \text{Im } A_{\chi^\pm}(K) + \text{Im } A_{\tilde{g}}(K) \right] , \qquad (38)$$

where, again by inspection with the SM expression for $|\epsilon|$ given in Eq. (10), one has

$$\text{Im } A_{SM}(K) = A^2\lambda^6\eta(y_c \left\{ \hat{\eta}_{ct}f_3(y_c, y_t) - \hat{\eta}_{cc} \right\} + \hat{\eta}_{tt}y_t f_2(y_t)A^2\lambda^4(1-\rho)) \qquad (39)$$

The expressions for Im $A_{H^\pm}(K)$, Im $A_{\chi^\pm}(B)$ and Im $A_{\tilde{g}}(B)$ can be found in Refs. [46, 54, 58].

For the analysis reported here, we follow the scenario called *minimal flavour violation* in Ref. [6]. In this class of supersymmetric theories, apart from the SM degrees of freedom, only charged Higgses, charginos and a light stop (assumed to be right-handed) contribute, with all other supersymmetric particles integrated out. This scenario is effectively implemented in a class of SUGRA models (both minimal and non-minimal) and gauge-mediated models [59], in which the first two squark generations are heavy and the contribution from the intermediate gluino-squark states is small [45, 54, 55, 56, 57].

For these models, the next-to-leading-order (NLO) corrections for ΔM_d, ΔM_s and $|\epsilon|$ can be found in Ref. [7]. Moreover, the branching ratio $\mathcal{B}(B \rightarrow X_s\gamma)$ has been calculated in Ref. [6]. We make use of this information and quantitatively examine the unitarity triangle, CP-violating asymmetries and their correlations for this class of supersymmetric theories. The phenomenological profiles of the unitarity triangle and CP phases for the SM and this class of supersymmetric models can thus be meaningfully compared. Given the high precision on the phases α, β and γ expected from experiments at B-factories and hadron colliders, a quantitative comparison of this kind could provide a means of discriminating between the SM and this class of MSSM's.

The NLO QCD-corrected effective Hamiltonian for $\Delta B = 2$ transitions in the minimal flavour violation SUSY framework can be expressed as follows [7]:

$$H_{eff} = \frac{G_F^2}{4\pi^2}(V_{td}V_{tb}^*)^2 \hat{\eta}_{2,S}(B) S O_{LL} , \qquad (40)$$

where the NLO QCD correction factor $\hat{\eta}_{2,S}(B)$ is given by [7]:

$$\hat{\eta}_{2,S}(B) = \alpha_s(m_W)\gamma^{(0)}/(2\beta_{n_f}^{(0)}) \left[1 + \frac{\alpha_s(m_W)}{4\pi}\left(\frac{D}{S} + Z_{n_f} \right) \right] , \qquad (41)$$

in which n_f is the number of active quark flavours (here $n_f = 5$), and the quantities Z_{n_f}, $\gamma^{(0)}$ and $\beta_{n_f}^{(0)}$ are defined below. The operator $O_{LL} = O_1$ is the one which is present in the SM, previously defined in the discussion following Eq. (35). The explicit expression for the function S can be obtained from Ref. [58] and for D it is given in Ref. [7], where it is derived in the NDR (naive dimensional regularization) scheme using $\overline{MS}$-renormalization.

The Hamiltonian given above for B_d^0–$\overline{B}_d^0$ mixing leads to the mass difference

$$\Delta M_d = \frac{G_F^2}{6\pi^2}(V_{td}V_{tb}^*)^2 \hat{\eta}_{2,S}(B) S(f_{B_d}^2 \hat{B}_{B_d}) . \qquad (42)$$

The corresponding expression for ΔM_s is obtained by making the appropriate replacements. Since the QCD correction factors are identical for ΔM_d and ΔM_s, it follows that the quantities ΔM_d and ΔM_s are enhanced by the same factor in minimal flavour violation supersymmetry, as compared to their SM values, but the ratio $\Delta M_s/\Delta M_d$ in this theory is the same as in the SM.

The NLO QCD-corrected Hamiltonian for $\Delta S = 2$ transitions in the minimal flavour violation supersymmetric framework has also been obtained in Ref. [7]. From this, the result for ϵ can be written as:

$$|\epsilon| = \frac{G_F^2 f_K^2 M_K M_W^2}{6\sqrt{2}\pi^2 \Delta M_K}\hat{B}_K \left(A^2\lambda^6\eta \right) (y_c \{\hat{\eta}_{ct} f_3(y_c, y_t) - \hat{\eta}_{cc}\}$$
$$+ \hat{\eta}_2(K) S A^2\lambda^4(1-\rho)), \qquad (43)$$

where the NLO QCD correction factor is [7]:

$$\hat{\eta}_2(K) = \alpha_s(m_c)^{\gamma^{(0)}/(2\beta_3^{(0)})} \left(\frac{\alpha_s(m_b)}{\alpha_s(m_c)} \right)^{\gamma^{(0)}/(2\beta_4^{(0)})} \left(\frac{\alpha_s(M_W)}{\alpha_s(m_b)} \right)^{\gamma^{(0)}/(2\beta_5^{(0)})}$$
$$\left[1 + \frac{\alpha_s(m_c)}{4\pi}(Z_3 - Z_4) + \frac{\alpha_s(m_b)}{4\pi}(Z_4 - Z_5) + \frac{\alpha_s(M_W)}{4\pi}(\frac{D}{S} + Z_5) \right] . \qquad (44)$$

17

Here

$$Z_{n_f} = \frac{\gamma_{n_f}^{(1)}}{2\beta_{n_f}^{(0)}} - \frac{\gamma^{(0)}}{2\beta_{n_f}^{(0)2}}\beta_{n_f}^{(1)} \ , \tag{45}$$

and the quantities entering in Eqs. (41) and (44) are the coefficients of the well-known beta function and anomalous dimensions in QCD:

$$\gamma^{(0)} = 6\frac{N_c - 1}{N_c}, \quad \beta_{n_f}^{(0)} = \frac{11N_c - 2n_f}{3} \ ,$$

$$\beta_{n_f}^{(1)} = \frac{34}{3}N_c^2 - \frac{10}{3}N_c n_f - 2C_f n_f \ ,$$

$$\gamma_{n_f}^{(1)} = \frac{N_c - 1}{2N_c}\left[-21 + \frac{57}{N_c} - \frac{19}{3}N_c + \frac{4}{3}n_f\right] \ , \tag{46}$$

with $N_c = 3$ and $C_F = 4/3$. The ratio

$$\frac{\hat{\eta}_{2,S}(B)(NLO)}{\hat{\eta}_{2,S}(B)(LO)} = 1 + \frac{\alpha_s(M_W)}{4\pi}(\frac{D}{S} + Z_5), \tag{47}$$

is worked out numerically in Ref. [7] as a function of the supersymmetric parameters (chargino mass m_{χ_2}, mass of the lighter of the two stops $m_{\tilde{t}_R}$, and the mixing angle ϕ in the stop sector). This ratio is remarkably stable against variations in the mentioned parameters and is found numerically to be about 0.89. Since in the LO approximation the QCD correction factor $\hat{\eta}_{2,S}(B)(LO)$ is the same in the SM and SUSY, with

$$\hat{\eta}_{2,S}(B)(LO) = \alpha_s(M_W)^{\gamma^{(0)}/2\beta_{n_f}^{(0)}} \ , \tag{48}$$

the QCD correction factor $\hat{\eta}_{2,S}(B)(NLO)$ entering in the expressions for ΔM_d and ΔM_s in the MSSM is found to be $\hat{\eta}_{2,S}(B)(NLO) = 0.51$ in the $\overline{MS}$-scheme. This is to be compared with the corresponding quantity $\hat{\eta}_B = 0.55$ in the SM. Thus, NLO corrections in ΔM_d (and ΔM_s) are similar in the SM and MSSM, but not identical.

The expression for $\hat{\eta}_{2,S}(K)(NLO)/\hat{\eta}_{2,S}(K)(LO)$ can be expressed in terms of the ratio $\hat{\eta}_{2,S}(B)(NLO)/\hat{\eta}_{2,S}(B)(LO)$ given above and the flavour-dependent matching factors Z_{n_f}:

$$\frac{\hat{\eta}_{2,S}(K)(NLO)}{\hat{\eta}_{2,S}(K)(LO)} = \frac{\hat{\eta}_{2,S}(B)(NLO)}{\hat{\eta}_{2,S}(B)(LO)} + \frac{\alpha_s(m_c)}{4\pi}(Z_3 - Z_4) + \frac{\alpha_s(m_b)}{4\pi}(Z_4 - Z_5) \simeq 0.884 \ , \tag{49}$$

where we have used the numerical value $\hat{\eta}_{2,S}(B)(NLO)/\hat{\eta}_{2,S}(B)(LO) = 0.89$ calculated by Krauss and Soff [7], along with $\alpha_s(m_c) = 0.34$ and $\alpha_s(m_b) = 0.22$. Using the expression for the quantity $\hat{\eta}_{2,S}(K)(LO)$, which is given by the prefactor multiplying the square bracket in Eq. (44), one gets $\hat{\eta}_{2,S}(K)(NLO) = 0.53$ in the $\overline{MS}$-scheme. This is to be compared with the corresponding QCD correction factor in the SM, $\hat{\eta}_{tt} = 0.57$, given in Table 1. Thus the two NLO factors are again very similar but not identical.

Following the above discussion, the SUSY contributions to ΔM_d, ΔM_s and $|\epsilon|$ in supersymmetric theories are incorporated in our analysis in a simple form:

$$\Delta M_d = \Delta M_d(SM)[1 + f_d(m_{\chi_2^\pm}, m_{\tilde{t}_R}, m_{H^\pm}, \tan v)],$$

$$\Delta M_s = \Delta M_s(SM)[1 + f_s(m_{\chi_2^\pm}, m_{\tilde{t}_R}, m_{H^\pm}, \tan \upsilon)],$$

$$|\epsilon| = \frac{G_F^2 f_K^2 M_K M_W^2}{6\sqrt{2}\pi^2 \Delta M_K} \hat{B}_K \left(A^2\lambda^6\eta\right) (y_c \{\hat{\eta}_{ct} f_3(y_c, y_t) - \hat{\eta}_{cc}\}$$
$$+ \hat{\eta}_{tt} y_t f_2(y_t)[1 + f_\epsilon(m_{\chi_2^\pm}, m_{\tilde{t}_2}, m_{H^\pm}, \tan \upsilon)]A^2\lambda^4(1 - \rho)). \tag{50}$$

The quantities f_d, f_s and f_ϵ can be expressed as

$$f_d = f_s = \frac{\hat{\eta}_{2,S}(B)}{\hat{\eta}_B} R_{\Delta_d}(S),$$

$$f_\epsilon = \frac{\hat{\eta}_{2,S}(K)}{\hat{\eta}_{tt}} R_{\Delta_d}(S), \tag{51}$$

where $R_{\Delta_d}(S)$ is defined as

$$R_{\Delta_d}(S) \equiv \frac{\Delta M_d(SUSY)}{\Delta M_d(SM)}(LO) = \frac{S}{y_t f_2(y_t)} . \tag{52}$$

The functions f_i, $i = d, s, \epsilon$ are all positive definite, i.e. the supersymmetric contributions add *constructively* to the SM contributions in the entire allowed supersymmetric parameter space. We find that the two QCD correction factors appearing in Eq. (51) are numerically very close to one another, with $\hat{\eta}_{2,S}(B)/\hat{\eta}_B \simeq \hat{\eta}_{2,S}(K)/\hat{\eta}_{tt} = 0.93$. Thus, to an excellent approximation, one has $f_d = f_s = f_\epsilon \equiv f$.

How big can f be? This quantity is a function of the masses of the top squark, chargino and the charged Higgs, $m_{\tilde{t}_R}$, $m_{\tilde{\chi}_2^\pm}$ and $m_{H^\pm}$, respectively, as well as of $\tan \upsilon$. The maximum allowed value of f depends on the model (minimal SUGRA, non-minimal SUGRA, MSSM with constraints from EDMs, etc.). We have numerically calculated the quantity f by varying the SUSY parameters ϕ, $m_{\tilde{t}_R}$, m_{χ_2}, $m_{H^\pm}$ and $\tan \upsilon$. Using, for the sake of illustration, $m_{\chi_2^\pm} = m_{\tilde{t}_R} = m_{H^\pm} = 100$ GeV, $m_{\chi_1^\pm} = 400$ GeV and $\tan \upsilon = 2$, and all other supersymmetric masses much heavier, of $O(1)$ TeV, we find that the quantity f varies in the range:

$$0.4 \le f \le 0.75 \quad \text{for} \quad |\phi| \le \pi/4 , \tag{53}$$

with the maximum value of f being at $\phi = 0$. These parametric values are allowed by the constraints from the NLO analysis of the decay $B \to X_s + \gamma$ reported in Ref. [6], as well as from direct searches of the supersymmetric particles [8]. The allowed range of f is reduced as $\tan \upsilon$ increases. Thus, for $\tan \upsilon = 4$, one has $0.15 \le f \le 0.42$ for $|\phi| \le \pi/4$. Likewise, f decreases as $m_{\tilde{t}_R}$, m_{χ_2} and $m_{H^\pm}$ increase, though the dependence of f on $m_{H^\pm}$ is rather mild due to the compensating effect of the $H^\pm$ and chargino contributions in the MSSM, as observed in Ref. [6]. This sets the size of f allowed by the present constraints in the minimal flavour violation version of the MSSM.

If additional constraints on the supersymmetry breaking parameters are imposed, as is the case in the minimal and non-minimal versions of the SUGRA models, then the allowed values of f will be further restricted. A complete NLO analysis of f would require a monte-carlo approach implementing all the experimental and theoretical constraints (such as the SUGRA-type mass relations). In particular, the NLO correlation between $\mathcal{B}(B \to X_s\gamma)$ and f has to

be studied in an analogous fashion, as has been done, for example, in Refs. [56, 57] with the leading order SUSY effects.

In this paper we adopt an approximate method to constrain f in SUGRA-type models. We take the maximum allowed values of the quantity $R_{\Delta_d}(S)$, defined earlier, from the existing LO analysis of the same and obtain f by using Eq. (51). For the sake of definiteness, we use the updated work of Goto et al. [56, 57], which is based, among other constraints, on the following:

- The lightest chargino mass is larger than 91 GeV, and all other charged SUSY particle masses are larger than 80 GeV.

- The gluino and squark masses are bounded from the searches at TEVATRON and LEP [8].

- Constraints on the supersymmetric parameters taking into account the NLO calculation of the decay branching ratio $\mathcal{B}(B \to X_s \gamma)$ in the SM and the charged Higgs contribution in the MSSM [60], and the updated experimental branching ratio from the CLEO and ALEPH collaborations, which at 95% C.L. is given by

$$2.0 \times 10^{-4} \leq \mathcal{B}(B \to X_s \gamma) \leq 4.5 \times 10^{-4} \ . \tag{54}$$

This last constraint plays a rather crucial role in determining the allowed values of $R_{\Delta_d}(S)$ — and hence of $\Delta M_d(SUSY)/\Delta M_d(SM)$ and $|\epsilon|(SUSY)/|\epsilon|(SM)$ — as the magnitude of the SUSY contribution in ΔM_d, $|\epsilon|$ and $\mathcal{B}(B \to X_s \gamma)$ are strongly correlated for the small $\tan \upsilon$ case [56, 57]. In fact, were it not for the bounds on $\mathcal{B}(B \to X_s \gamma)$ given above, much larger values of $R_{\Delta_d}(S)$ would be allowed.

From the published results we conclude that typically f can be as large as 0.45 in non-minimal SUGRA models for low $\tan \upsilon$ (typically $\tan \upsilon = 2$) [56], and approximately half of this value in minimal SUGRA models [45, 55, 56]. Relaxing the SUGRA mass constraints, admitting complex values of A and μ but incorporating the EDM constraints, and imposing the constraints mentioned above, Baek and Ko [49] find that f could be as large as $f = 0.75$. In all cases, the value of f decreases with increasing $\tan \upsilon$ or increasing $m_{\tilde{\chi}_2^\pm}$ and $m_{\tilde{t}_R}$, as noted above.

3.3 SUSY Fits

For the SUSY fits, we use the same program as for the SM fits, except that the theoretical expressions for ΔM_d, ΔM_s and $|\epsilon|$ are modified as in Eq. (50). We compare the fits for four representative values of the SUSY function f — 0, 0.2, 0.4 and 0.75 — which are typical of the SM, minimal SUGRA models, non-minimal SUGRA models, and non-SUGRA models with EDM constraints, respectively.

The allowed 95% C.L. regions for these four values of f are all plotted in Fig. 6. As is clear from this figure, there is still a considerable overlap between the $f = 0$ (SM) and $f = 0.75$ regions. However, there are also regions allowed for one value of f which are excluded for
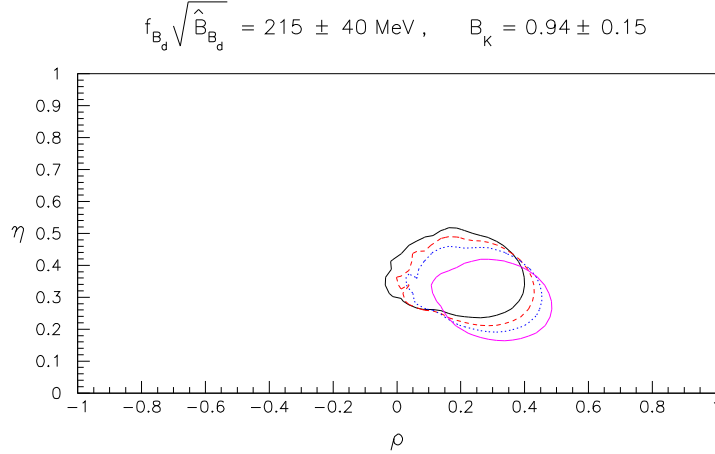
$$f_{B_d}\sqrt{\hat{B}_{B_d}} = 215 \pm 40 \text{ MeV}, \qquad B_K = 0.94 \pm 0.15$$

Figure 6: Allowed 95% C.L. region in ρ–η space in the SM and in SUSY models, from a fit to the data given in Table 1. From left to right, the allowed regions correspond to $f = 0$ (SM, solid line), $f = 0.2$ (long dashed line), $f = 0.4$ (short dashed line), $f = 0.75$ (dotted line).

another value. Thus a sufficiently precise determination of the unitarity triangle might be able to exclude certain values of f (including the SM, $f = 0$).

From Fig. 6 it is clear that a measurement of the CP angle β will *not* distinguish among the various values of f: even with the naked eye it is evident that the allowed range for β is roughly the same for all models. Rather, it is the measurement of γ or α which has the potential to rule out certain values of f. As f increases, the allowed region moves slightly down and towards the right in the ρ–η plane, corresponding to smaller values of γ (or equivalently, larger values of α). We illustrate this in Table 2, where we present the allowed ranges of α, β and γ, as well as their central values (corresponding to the preferred values of ρ and η), for each of the four values of f. From this Table, we see that the allowed range of β is largely insensitive to the model. Conversely, the allowed values of α and γ do depend somewhat strongly on the chosen value of f. Note, however, that one is not guaranteed to be able to distinguish among the various models: as mentioned above, there is still significant overlap among all four models. Thus, depending on what values of α and γ are obtained, we may or may not be able to rule out certain values of f.

One point which is worth emphasizing is the correlation of γ with f. This study clearly shows that large values of f require smaller values of γ. The reason that this is important is as follows. The allowed range of γ for a particular value of f is obtained from a fit to all CKM data, even those measurements which are unaffected by the presence of supersymmetry. Now, the size of γ indirectly affects the branching ratio for $B \to X_s \gamma$: a larger value of γ corresponds to a smaller value of $|V_{ts}|$ through CKM unitarity. And this branching ratio is among the experimental data used to bound SUSY parameters and calculate the allowed range of f. Therefore, the above γ–f correlation indirectly affects the allowed values of f in a particular SUSY model, and thus must be taken into account in studies which examine the range of f. For example, it is often the case that larger values of f are allowed for large values of γ. However, as we have seen above, the CKM fits disfavour such values of γ.

21

f	α	β	γ	$(\alpha, \beta, \gamma)_{\text{cent}}$
$f = 0$ (SM)	$65° - 123°$	$16° - 35°$	$36° - 97°$	$(93°, 25°, 62°)$
$f = 0.2$	$70° - 129°$	$16° - 34°$	$32° - 90°$	$(102°, 24°, 54°)$
$f = 0.4$	$75° - 134°$	$15° - 34°$	$28° - 85°$	$(110°, 23°, 47°)$
$f = 0.75$	$86° - 141°$	$13° - 33°$	$23° - 73°$	$(119°, 22°, 39°)$

Table 2: Allowed 95% C.L. ranges for the CP phases α, β and γ, as well as their central values, from the CKM fits in the SM ($f = 0$) and supersymmetric theories, characterized by the parameter f defined in the text.

f	$\sin 2\alpha$	$\sin 2\beta$	$\sin^2 \gamma$
$f = 0$ (SM)	$-0.91 - 0.77$	$0.53 - 0.94$	$0.35 - 1.00$
$f = 0.2$	$-0.98 - 0.65$	$0.52 - 0.93$	$0.28 - 1.00$
$f = 0.4$	$-1.00 - 0.50$	$0.49 - 0.93$	$0.22 - 0.99$
$f = 0.75$	$-1.00 - 0.14$	$0.45 - 0.91$	$0.16 - 0.91$

Table 3: Allowed 95% C.L. ranges for the CP asymmetries $\sin 2\alpha$, $\sin 2\beta$ and $\sin^2 \gamma$, from the CKM fits in the SM ($f = 0$) and supersymmetric theories, characterized by the parameter f defined in the text.

For completeness, in Table 3 we present the corresponding allowed ranges for the CP asymmetries $\sin 2\alpha$, $\sin 2\beta$ and $\sin^2 \gamma$. Again, we see that the allowed range of $\sin 2\beta$ is largely independent of the value of f. On the other hand, as f increases, the allowed values of $\sin 2\alpha$ become increasingly negative, while those of $\sin^2 \gamma$ become smaller.

The allowed (correlated) values of the CP angles for various values of f can be clearly seen in Figs. 4 and 5. As f increases from 0 (SM) to 0.75, the change in the allowed $\sin 2\alpha$–$\sin 2\beta$ (Fig. 4) and α–γ (Fig. 5) regions is quite significant.

In Sec. 2.1, we noted that $|V_{ub}/V_{cb}|$, $\hat{B}_K$ and $f_{B_d}\sqrt{\hat{B}_{B_d}}$ are very important in defining the allowed region in the ρ–η plane. At present, these three quantities have large errors, which are mostly theoretical in nature. Let us suppose that our theoretical understanding of these quantities improves, so that the errors are reduced by a factor of two, i.e.

$$\left| \frac{V_{ub}}{V_{cb}} \right| = 0.093 \pm 0.007 \ ,$$
$$\hat{B}_K = 0.94 \pm 0.07 \ ,$$
$$f_{B_d}\sqrt{\hat{B}_{B_d}} = 215 \pm 20 \text{ MeV} \ . \tag{55}$$

How would such an improvement affect the SUSY fits?

We present the allowed 95% C.L. regions ($f = 0, 0.2, 0.4, 0.75$) for this hypothetical situation in Fig. 7. Not surprisingly, the regions are quite a bit smaller than in Fig. 6. More importantly for our purposes, the regions for the different values of f have become more separated from one another. That is, although there is still a region where all four f values are allowed, precise measurements of the CP angles have a better chance of ruling out certain values of f.
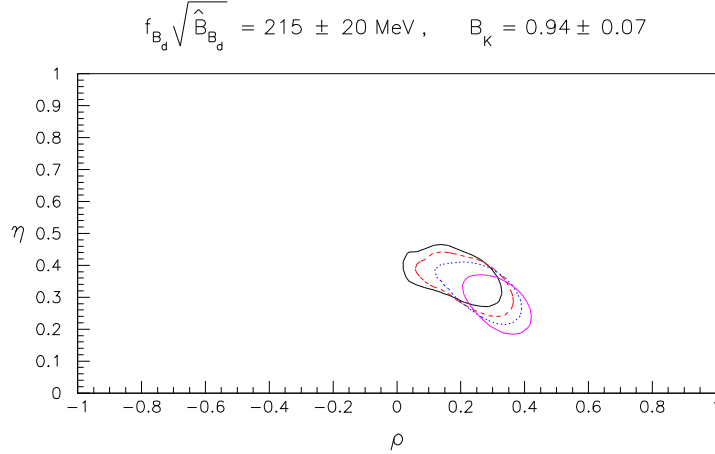
$$f_{B_d}\sqrt{\hat{B}_{B_d}} = 215 \pm 20 \text{ MeV}, \quad B_K = 0.94 \pm 0.07$$

Figure 7: Allowed 95% C.L. region in ρ–η space in the SM and in SUSY models, from a fit to the data given in Table 1, with the (hypothetical) modifications given in Eq. (55). From left to right, the allowed regions correspond to $f = 0$ (SM, solid line), $f = 0.2$ (long dashed line), $f = 0.4$ (short dashed line), $f = 0.75$ (dotted line).

In Table 4 we present the allowed ranges of α, β and γ, as well as their central values, for this scenario. Table 5 contains the corresponding allowed ranges for the CP asymmetries $\sin 2\alpha$, $\sin 2\beta$ and $\sin^2 \gamma$. The allowed $\sin 2\alpha$–$\sin 2\beta$ and α–γ correlations are shown in Figs. 8 and 9, respectively. As is consistent with the smaller regions of Fig. 6, the allowed (correlated) regions are considerably reduced compared to Figs. 4 and 5. As before, although the measurement of β will not distinguish among the various values of f, the measurement of α or γ may.

Indeed, the assumed reduction of errors in Eq. (55) increases the likelihood of this happening. For example, consider again Table 2, which uses the original data set of Table 1. Here we see that $65° \leq \alpha \leq 123°$ for $f = 0$ and $86° \leq \alpha \leq 141°$ for $f = 0.75$. Thus, if experiment finds α in the range $86°$–$123°$, one cannot distinguish the SM ($f = 0$) from the SUSY model with $f = 0.75$. However, consider now Table 4, obtained using data with reduced errors. Here, $67° \leq \alpha \leq 116°$ for $f = 0$ and $97° \leq \alpha \leq 137°$ for $f = 0.75$. Now, it is only if experiment finds α in the range $97°$–$116°$ that one cannot distinguish $f = 0$ from $f = 0.75$. But this range is quite a bit smaller than that obtained using the original data. This shows how an improvement in the precision of the data can help not only in establishing the presence of new physics, but also in distinguishing among various models of new physics.

4   Conclusions

In the very near future, CP-violating asymmetries in B decays will be measured at B-factories, HERA-B and hadron colliders. Such measurements will give us crucial information about the interior angles α, β and γ of the unitarity triangle. If we are lucky, there will be an inconsistency in the independent measurements of the sides and angles of this triangle, thereby revealing the presence of new physics.
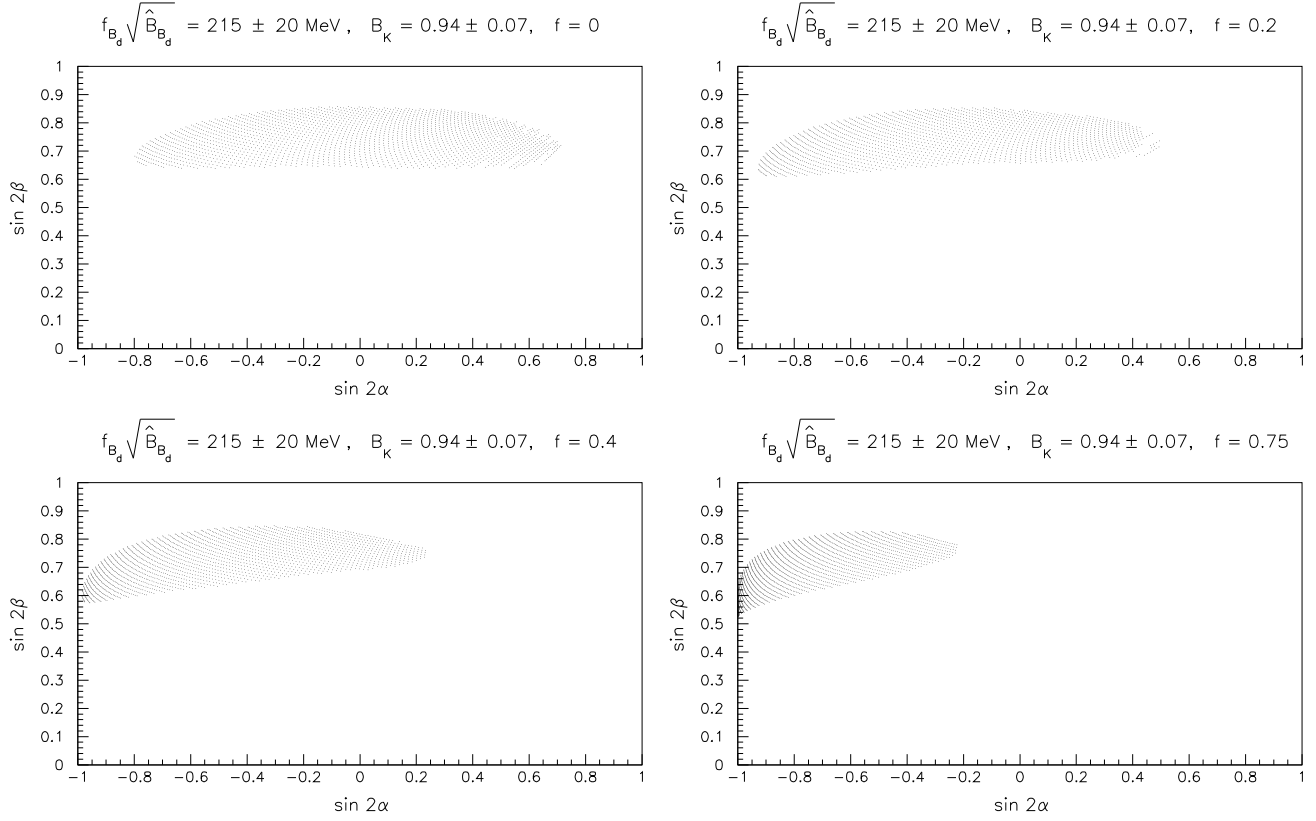
Figure 8: Allowed 95% C.L. region of the CP-violating quantities $\sin 2\alpha$ and $\sin 2\beta$, from a fit to the data given in Table 1, with the (hypothetical) modifications given in Eq. (55). The upper left plot ($f = 0$) corresponds to the SM, while the other plots ($f = 0.2$, 0.4, 0.75) correspond to various SUSY models.

f	α	β	γ	$(\alpha, \beta, \gamma)_{\rm cent}$
$f = 0$ (SM)	$67° - 116°$	$20° - 30°$	$42° - 90°$	$(93°, 24°, 63°)$
$f = 0.2$	$74° - 124°$	$19° - 29°$	$36° - 82°$	$(102°, 24°, 54°)$
$f = 0.4$	$83° - 130°$	$18° - 29°$	$31° - 73°$	$(110°, 23°, 47°)$
$f = 0.75$	$97° - 137°$	$16° - 28°$	$26° - 59°$	$(119°, 22°, 39°)$

Table 4: Allowed 95% C.L. ranges for the CP phases α, β and γ, as well as their central values, from the CKM fits in the SM ($f = 0$) and supersymmetric theories, characterized by the parameter f defined in the text. We use the data given in Table 1, with the (hypothetical) modifications given in Eq. (55).
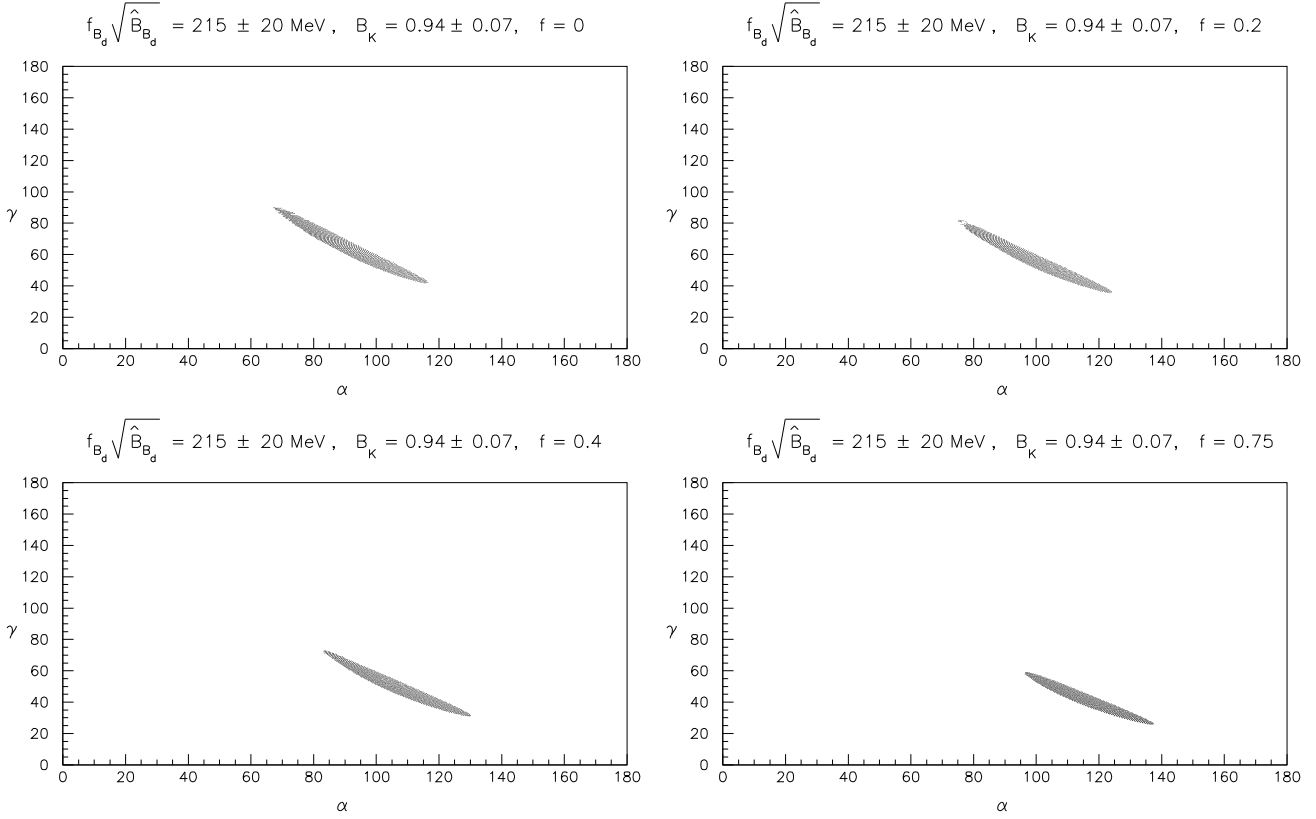
24

Figure 9: Allowed 95% C.L. region of the CP-violating quantities α and γ, from a fit to the data given in Table 1, with the (hypothetical) modifications given in Eq. (55). The upper left plot ($f = 0$) corresponds to the SM, while the other plots ($f = 0.2$, 0.4, 0.75) correspond to various SUSY models.

f	$\sin 2\alpha$	$\sin 2\beta$	$\sin^2 \gamma$
$f = 0$ (SM)	$-0.80 - 0.71$	$0.64 - 0.86$	$0.44 - 1.00$
$f = 0.2$	$-0.93 - 0.53$	$0.61 - 0.85$	$0.34 - 0.98$
$f = 0.4$	$-0.99 - 0.23$	$0.57 - 0.85$	$0.27 - 0.91$
$f = 0.75$	$-1.00 - -0.23$	$0.52 - 0.83$	$0.19 - 0.73$

Table 5: Allowed 95% C.L. ranges for the CP asymmetries $\sin 2\alpha$, $\sin 2\beta$ and $\sin^2 \gamma$, from the CKM fits in the SM ($f = 0$) and supersymmetric theories, characterized by the parameter f defined in the text. We use the data given in Table 1, with the (hypothetical) modifications given in Eq. (55).

25

If present, this new physics will affect B decays principally through new contributions to B^0–$\overline{B^0}$ mixing. If these contributions come with new phases (relative to the SM), then the CP asymmetries can be enormously shifted from their SM values. In this case there can be huge discrepancies between measurements of the angles and the sides, so that the new physics will be easy to find.

In fact, there are several models which have new contributions, with new phases, to B^0–$\overline{B^0}$ mixing. However, these models do not predict what those phases are. That is, there are no *predictions* for the values of CP asymmetries in such models. All that can be said is that large effects are possible.

A more interesting possibility, from the point of view of making predictions, are models which contribute to B^0–$\overline{B^0}$ mixings and $|\epsilon|$, but without new phases. One type of new physics which does just this is supersymmetry (SUSY). There are some SUSY models which do contain new phases, but they suffer from the problem described above: lack of predictivity. However, there is also a large class of SUSY models with no new phases. In this paper we have concentrated on these models.

There has been an enormous amount of study of SUSY models over the past two decades. Much of this work has concentrated on the minimal supersymmetric standard model (MSSM), in which the new phases are constrained by limits on the electric dipole moments of the neutron and electron to be essentially zero. Taking into account supersymmetry breaking, in supergravity (SUGRA) models, the SUSY-breaking parameters of the MSSM are assumed to take a simple form at the Planck scale. However, there are a variety of ways to do this, so that in fact there is a fairly large class of SUSY models in which there are new contributions to B^0–$\overline{B^0}$ mixing, but no new phases.

In this paper we have examined the predictions of such models for the unitarity triangle and explored the extent to which this type of new physics can be discovered through measurements of the sides and angles of the unitarity triangle.

In these models, there are new, supersymmetric contributions to K^0–$\overline{K^0}$, B_d^0–$\overline{B_d^0}$ and B_s^0–$\overline{B_s^0}$ mixing. The key ingredient in our analysis is the fact that these contributions, which add constructively to the SM, depend on the SUSY parameters in essentially the same way. That is, so far as an analysis of the unitarity triangle is concerned, there is a single parameter, f, which characterizes the various SUSY models within this class of models ($f = 0$ corresponds to the SM). For example, the values $f = 0.2$, 0.4 and 0.75 are found in minimal SUGRA models, non-minimal SUGRA models, and non-SUGRA models with EDM constraints, respectively.

We have therefore updated the profile of the unitarity triangle in both the SM and some variants of the MSSM. We have used the latest experimental data on $|V_{cb}|$, $|V_{ub}/V_{cb}|$, ΔM_d and ΔM_s, as well as the latest theoretical estimates (including errors) of $\hat{B}_K$, $f_{B_d}\sqrt{\hat{B}_{B_d}}$ and $\xi_s \equiv f_{B_d}\sqrt{\hat{B}_{B_d}}/f_{B_s}\sqrt{\hat{B}_{B_s}}$. In addition to $f = 0$ (SM), we considered the three SUSY values of f: 0.2, 0.4 and 0.75.

We first considered the profile of the unitarity triangle in the SM, shown in Fig. 2. At present, the allowed ranges for the CP angles at 95% C.L. are

$$65° \leq \alpha \leq 123° \quad , \quad 16° \leq \beta \leq 35° \quad , \quad 36° \leq \gamma \leq 97° \quad , \tag{56}$$

or equivalently,

$$-0.91 \le \sin 2\alpha \le 0.77 \quad , \quad 0.52 \le \sin 2\beta \le 0.94 \quad , \quad 0.35 \le \sin^2 \gamma \le 1.00 \quad . \qquad (57)$$

We then compared the SM with the different SUSY models. The result can be seen in Fig. 6. As f increases, the allowed region moves slightly down and to the right in the ρ–η plane. The main conclusion from this analysis is that the measurement of the CP angle β will not distinguish among the SM and the various SUSY models – the allowed region of β is virtually the same in all these models. On the other hand, the allowed ranges of α and γ do depend on the choice of f. For example, larger values of f tend to favour smaller values of γ. Thus, with measurements of γ or α, we may be able to rule out certain values of f (including the SM, $f = 0$). However, we also note that there is no guarantee of this happening – at present there is still a significant region of overlap among all four models.

Finally, we also considered a hypothetical future data set in which the errors on $|V_{ub}/V_{cb}|$, $\hat{B}_K$ and $f_{B_d}\sqrt{\hat{B}_{B_d}}$, which are mainly theoretical, are reduced by a factor of two. For two of these quantities ($|V_{ub}/V_{cb}|$ and $f_{B_d}\sqrt{\hat{B}_{B_d}}$), this has the effect of reducing the uncertainty on the sides of the unitarity triangle by the same factor. The comparison of the SM and SUSY models is shown in Fig. 7. As expected, the allowed regions for all models are quite a bit smaller than before. Furthermore, the regions for different values of f have become more separated, so that precise measurements of the CP angles have a better chance of ruling out certain values of f.

Note added: As we were submitting this paper for publication, we noted the preprint by F. Parodi, P. Roudeau and A. Stocchi (LAL 99-03, DELPHI 99-27 CONF 226, hep-ex/9903063), in which the constraints on the parameters of the CKM matrix are presented in the SM. Though our input parameters differ, in particular the assumed errors, our results in the SM are similar to theirs but not identical.

References

[1] N. Cabibbo, Phys. Rev. Lett. **10** (1963) 531; M. Kobayashi and K. Maskawa, Prog. Theor. Phys. **49** (1973) 652.

[2] L. Wolfenstein, Phys. Rev. Lett. **51** (1983) 1945.

[3] For reviews, see, for example, Y. Nir and H. R. Quinn in *B Decays*, edited by S. Stone (World Scientific, Singapore, 1994), p. 362; I. Dunietz, *ibid.*, p. 393; M. Gronau, *Proceedings of Neutrino 94, XVI International Conference on Neutrino Physics and Astrophysics*, Eilat, Israel, May 29 – June 3, 1994, eds. A. Dar, G. Eilam and M. Gronau, Nucl. Phys. (Proc. Suppl.) **B38** (1995) 136.

[4] C.O. Dib, D. London and Y. Nir, Int. J. Mod. Phys. **A6** (1991) 1253.

[5] For a review of new-physics effects in CP asymmetries in the *B* system, see M. Gronau and D. London, Phys. Rev. **D55** (1997) 2845, and references therein.

[6] M. Ciuchini, G. Degrassi, P. Gambino and G.F. Giudice, Nucl. Phys. **B534** (1998) 3.

[7] F. Krauss and G. Soff, preprint hep-ph/9807238.

[8] C. Caso et al. (Particle Data Group), Eur. Phys. J. **C3** (1998) 1.

[9] M. Neubert, in *Heavy Flavors*, Second Edition, edited by A.J. Buras and M. Lindner (World Scientific, Singapore, 1997) and hep-ph/9702375.

[10] A. Czarnecki and K. Melnikov, Phys. Rev. Lett. **78** (1997) 3630; Nucl. Phys. **B505** (1997) 65.

[11] M. Shifman, in *Proc.* PASCHOS 1995, Baltimore, Maryland, 22-25 March 1995 and hep-ph/9505289.

[12] F. Parodi, in *Proc.* of XXIXth. Int. Conf. on High Energy Physics, Vancouver, B.C., 1998.

[13] S. Mele, preprint CERN-EP/98-133, hep-ph/9810333 (1998).

[14] A.J. Buras, W. Slominski, and H. Steger, Nucl. Phys. **B238** (1984) 529; *ibid.* **B245** (1984) 369.

[15] T. Inami and C.S. Lim, Progr. Theor. Phys. **65** (1981) 297.

[16] S. Herrlich and U. Nierste, Nucl. Phys. **B419** (1994) 292.

[17] A.J. Buras, M. Jamin and P.H. Weisz, Nucl. Phys. **B347** (1990) 491.

[18] S. Herrlich and U. Nierste, Phys. Rev. **D52** (1995) 6505.

[19] T. Draper, preprint hep-lat/9810065 (1998).

[20] S. Sharpe, preprint hep-lat/9811006 (1998).

[21] J. Alexander, *in Proc.* of XXIXth. Int. Conf. on High Energy Physics, Vancouver, B.C., 1998.

[22] A. Ali and D. London, Z. Phys. **C65** (1995) 431; Nucl. Phys. Proc. Suppl. **54A** (1997) 297.

[23] C. Bernard et al., Phys. Rev. Lett. **81** (1998) 4812.

[24] H.G. Moser and A. Roussarie, Nucl. Instr. Meth. **A384** (1997) 491.

[25] Seminar presented by P. Shawhan (KTEV Collaboration), Fermilab, IL, Feb. 24, 1999; see also http://fnphyx-www.fnal.gov/experiments/ktev/epsprime/.

[26] G.D. Barr et al. (NA31 Collaboration), Phys. Lett. **B317** (1993) 233.

[27] L. Wolfenstein, Phys. Rev. Lett. **13** (1964) 380.

[28] A.J. Buras, M. Jamin and M.E. Lautenbacher, Nucl. Phys. **B370** (1992) 69; *ibid.* **B400** (1993) 37; *ibid.* **B400** (1993) 75; *ibid.* **B408** (1993) 209.

[29] M. Ciuchini et al., Phys. Lett. **B301** (1993) 263; Nucl. Phys. **B415** (1994) 403;

[30] S. Bertolini, M. Fabbrichesi and J.O. Egg, Nucl. Phys. **B499** (1995) 197; *ibid.* **B476** (1996) 225.

[31] A.J. Buras and L. Silvestrini, preprint TUM-HEP-334/98, hep-ph/9811471.

[32] For recent reviews, see R. Gupta, preprint hep-ph/9801412 and L. Conti et al., Phys. Lett. **B421** (1998) 273.

[33] W.A. Bardeen, A.J. Buras and J.M. Gerard, Phys. Lett. **B180** (1986) 133; Nucl. Phys. **B293** (1987) 787; Phys. Lett. **B192** (1987) 138; G.O. Köhler et al., Phys. Rev. **D58** (1998) 014017.

[34] A.J. Buras et al., preprint TUM-HEP-316-98, hep-ph/9806471.

[35] Y.-Y. Keum, U. Nierste and A.I. Sanda, preprint KEK-TH-612, FERMILAB-Pub-99/035-T, hep-ph/9903230.

[36] A. Masiero and H. Murayama, preprint hep-ph/9903363.

[37] CDF Collaboration, CDF/PUB/BOTTOM/CDF/4855.

[38] F. Parodi, P. Roudeau and A. Stocchi, preprint LAL 98-49, hep-ph/9802289.

[39] M. Gronau and D. Wyler, Phys. Lett. **B265** (1991) 172. See also M. Gronau and D. London, Phys. Lett. **B253** (1991) 483; I. Dunietz, Phys. Lett. **B270** (1991) 75. Improvements to this method have recently been discussed by D. Atwood, I. Dunietz and A. Soni, Phys. Rev. Lett. **78** (1997) 3257.

[40] R. Aleksan, I. Dunietz and B. Kayser, Z. Phys. **C54** (1992) 653.

[41] See, for example, H.P. Nilles, Phys. Rep. **110** (1984) 1.

[42] M. Dugan, B. Grinstein and L.J. Hall, Nucl. Phys. **B255** (1985) 413; S. Dimopoulos and S. Thomas, Nucl. Phys. **B465** (1996) 23.

[43] A.G. Cohen, D.B. Kaplan and A.E. Nelson, Phys. Lett. **B388** (1996) 588; A.G. Cohen, D.B. Kaplan, F. Lepeintre and A.E. Nelson, Phys. Rev. Lett. **78** (1997) 2300.

[44] T. Falk, K.A. Olive and M. Srednicki, Phys. Lett. **B354** (1995) 99; T. Falk and K.A. Olive, *ibid.* **B375** (1996) 196.

[45] T. Nihei, Prog. Theor. Phys. **98** (1997) 1157.

[46] G.C. Branco, G.C. Cho, Y. Kizukuri and N. Oshimo, Phys. Lett. **B337** (1994) 316; Nucl. Phys. **B449** (1995) 483.

[47] R. Contino and I. Scimemi, preprint ROME1-1216-98, hep-ph/9809437.

[48] D.A. Demir, A. Masiero and O. Vives, preprint SISSA/EP/140/98, IC/98/228, hep-ph/9812337.

[49] S. Baek and P. Ko, preprint KAIST-20/98, SNUTP 98-139, hep-ph/9812229.

[50] D. Chang, W.-Y. Keung and A. Pilaftsis, Phys. Rev. Lett. **82** (1999) 900.

[51] J.P. Silva and L. Wolfenstein, Phys. Rev. **D55** (1997) 5331.

[52] L. Randall and S. Su, Nucl. Phys. **B540** (1999) 37.

[53] M. Ciuchini et al., JHEP 9810: 008, 1998.

[54] T. Goto, T. Nihei and Y. Okada, Phys. Rev. **D53** (1996) 5233.

[55] T. Goto, Y. Okada, Y. Shimizu and M. Tanaka, Phys. Rev. **D55** (1997) 4273.

[56] T. Goto, Y. Okada and Y. Shimizu, Phys. Rev. **D58**: 094006 (1998); KEK-TH-611 (1999) (in preparation).

[57] T. Goto et al., preprint KEK-TH-608, KEK Preprint 98-206, hep-ph/9812369.

[58] S. Bertolini, F. Borzumati, A. Masiero and G. Ridolphi, Nucl. Phys. **B353** (1991) 591.

[59] M. Dine and A.E. Nelson, Phys. Rev. **D48** (1993) 1277; M. Dine, A.E. Nelson and Y. Shirman, Phys. Rev. **D51** (1995) 1362; M. Dine, A.E. Nelson, Y. Nir and Y. Shirman, Phys. Rev. **D53** (1996) 2658.

[60] M. Ciuchini, G. Degrassi, P. Gambino and G.F. Giudice, Nucl. Phys. **B527** (1998) 21; P. Ciafaloni, A. Romanino and A. Strumia, Nucl. Phys. **B524** (1998) 361; F. Borzumati and C. Greub, Phys. Rev. **D58** (1998) 74004, hep-ph/9809438; T.M. Aliev and E.O. Iltan, Phys. Rev. **D58** (1998) 95014.